FRAUNHOFER CHALMERS
RESEARCH CENTRE FOR INDUSTRIAL MATHEMATICS

DigiRail

High-Performance Computing for Construction, Operation and Maintenance of Railway Infrastructure

Final Summary Report

FCC Report 2026:01
August 2026

Vinnova: 2022-00167
Trafikverket: 2024/65940

FCC Report 2026:01

DigiRail

High-Performance Computing for Construction, Operation and Maintenance of Railway Infrastructure

Final Summary Report

Johannes Quist, Anita Ullrich, Pontus Malmsköld, Elias Börjesson, Caroline Ansin, Franziska Hunger, Clemens Steinke



FRAUNHOFER CHALMERS
RESEARCH CENTRE FOR INDUSTRIAL MATHEMATICS

Report Information

Title	DigiRail: High-Performance Computing for Construction, Operation and Maintenance of Railway Infrastructure
Authors	Johannes Quist, Anita Ullrich, Pontus Malmsköld, Elias Börjesson, Caroline Ansin, Franziska Hunger, Clemens Steinke
Report type	Final Summary Report
Publisher	Fraunhofer-Chalmers Centre for Industrial Mathematics
Publication no.	FCC Report 2026:01
Published	August 2026
Project	DigiRail
Coordinator	Fraunhofer-Chalmers Centre
Project leader	Johannes Quist
Project period	2022–2026
Vinnova programme	InfraSweden2030
Vinnova Reg. No.	2022-00167
Trafikverket FoI portfolio	FoI Portfolio Bygga
Trafikverket Reg. No.	2024/65940

Project and Funding Information

Project	DigiRail
Vinnova funding	InfraSweden2030, Reg. No. 2022-00167
Trafikverket funding	FoI Portfolio Bygga, Reg. No. 2024/65940
Coordinating organisation	Fraunhofer-Chalmers Centre
Project partners:	

Fraunhofer-Chalmers Centre
Dynapac Compaction Equipment
Infranord
Trafikverket
NCC
Volvo Construction Equipment
Ramboll

Preface

DigiRail has been a highly collaborative project, and the work presented in this report would not have been possible without the engagement, support and technical contributions from a large number of people and organisations.

I would first like to thank our partners at Volvo Construction Equipment: Elianne Lindmark, Manoranjan Kumar, Abdulkarim Habbab, Bobbie Frank and Per-Olof Danielsson. Their strong engagement throughout the project has been greatly appreciated. A particular thanks goes to Elianne and Manoranjan, and to Volvo CE for providing access to full-scale test environments and experimental data that have been essential for the validation work.

A very special thanks also goes to Andreas Persson, Mikael Knutsson, Maria Wilhelmsson, Fredrik Åkesson and Christoffer Brauer at Dynapac Compaction Equipment. Their support has been exceptional throughout the project, not least in connection with the extensive full-scale experimental work carried out in Karlskrona.

I would also like to thank Roland Bång and Jerker Sundström at Infranord. Roland has contributed invaluable input on railway maintenance, access to test environments and operational data, and an exceptional level of commitment throughout the project. We also acknowledge System7 for making operational tamping data and the Inframe environment available for the work.

At Ramboll, I would like to thank Tara Wood and Peter Simonsson, with a particular thanks to Tara for important feedback, discussions and many new ideas that have helped shape the work. I would also like to thank Alexandre Mathern at NCC Infrastructure, as well as Kristoffer Hofling and Christina Claeson-Jonsson at NCC Industry. Kristoffer has contributed valuable perspectives on ballast production and material behaviour, and has also been instrumental in the related spin-off activities carried out through SBUF projects.

A sincere thanks goes to Luleå University of Technology, Professor Gabriel Sas and his entire team. The collaboration has created strong scientific and technical synergies, and we very much look forward to continuing and developing this cooperation in future work.

I would also like to thank the DigiRail team at Fraunhofer-Chalmers Centre, in particular Anita Ullrich, Pontus Malmsköld, Elias Börjesson, Caroline Ansin, Franziska Hunger and Clemens Steinke. Their work on model development, implementation, simulation, validation and analysis forms the technical foundation of the work presented in this report. The breadth of DigiRail has required contributions across several modelling disciplines, and the commitment of the FCC team has been essential throughout the project.

We are also very grateful to SBUF for supporting complementary experimental and research activities that have significantly strengthened the project. Likewise, I would like to thank the InfraSweden2030 programme office for its continuous support throughout the project, including Fredrik, Camilla, Lisa and many others who have helped us along the way.

Finally, I would like to express my sincere thanks to Johan Jonsson and Thomas Asp at Trafikverket. Johan has been a strongly driving force in the project, and his technical ideas, commitment and ambition have had a major influence on how far the work has progressed. Without that engagement, the project would not have reached its present level.

To everyone who has contributed through experiments, modelling, discussions, reviews, data, project administration and practical support: thank you.

Johannes Quist
Project Leader, DigiRail
Fraunhofer-Chalmers Centre for Industrial Mathematics

Executive Summary

DigiRail has developed and validated a high-performance numerical framework for physics-based simulation of railway infrastructure across construction, operation and maintenance. The project addresses a central challenge in railway engineering: the track system consists of components with fundamentally different mechanical behaviour, ranging from granular ballast and unbound materials to rails, sleepers, supporting structures, vehicles and construction or maintenance machinery. Their interaction is important for phenomena such as settlement, load distribution, compaction, ballast degradation and the dynamic response of railway transition zones.

The developed framework combines the Discrete Element Method (DEM), Finite Element Method (FEM) and Multi-Body Dynamics (MBD). DEM is used to resolve the behaviour of ballast and other coarse granular materials at particle scale, FEM represents structural components and supporting continua, and MBD provides efficient representations of vehicles and machinery. The numerical methods are complemented by automated workflows for model generation, calibration, simulation management and execution on high-performance computing systems.

A coupled DEM–FEM railway model was developed as a common platform for the railway-specific investigations. The work included calibration of ballast behaviour, efficient generation of large ballast beds, realistic representations of non-spherical and non-convex particles, treatment of finite track boundaries, rail irregularities and dynamic moving loads. The studies showed that particle representation has a significant influence on calculated track behaviour: non-convex particles resulted in stronger geometric interlocking, higher track stiffness and reduced settlement compared with corresponding convex particle representations.

Experimental validation was performed at several scales. Coupled DEM–MBD simulations of full-scale vibratory roller compaction reproduced the principal evolution of settlement over 14 roller passes and important characteristics of measured ground pressure. The simulations additionally enabled the development of packing density through the depth of the granular layer to be investigated, providing information that is difficult to obtain experimentally.

The general DEM–MBD co-simulation methodology was also evaluated against full-scale wheel-loader experiments. The model captured important aspects of bucket filling, pile deformation and machine response for several operating sequences, while other cases identified limitations associated with the simplified machine representation. These results provide both validation of the coupling methodology and guidance for future model development.

Railway ballast behaviour was investigated using large-scale sleeper push tests, cyclic oedometer experiments and corresponding DEM simulations. The results demonstrated that particle size distribution affects deformation, stiffness and degradation, while confinement and vertical load strongly influence mobilised lateral resistance. The DEM simulations reproduced the main relative trends between the investigated materials and provided additional insight into particle rearrangement and force transmission.

At structural scale, DEM–FEM simulations were compared with measurements from a full-scale trough-bridge experiment. The simulations reproduced the general magnitude and spatial distribution of ballast-induced pressure and showed that different realizations of the granular bed can produce asymmetric local load patterns even under nominally symmetric loading. This illustrates the potential importance of the discrete and stochastic nature of ballast for structural load transfer.

A coupled DEM–MBD framework was further developed for railway tamping and calibrated against operational data from a fully hydraulic tamping machine. The investigated simulations indicate that machine concept and operating strategy can influence both the

achieved ballast packing state and the particle-scale force exposure. The work demonstrates the potential of detailed simulation for jointly considering maintenance effectiveness and ballast preservation, while additional validation and explicit particle-breakage modelling remain important future steps.

Finally, the railway model was applied to a transition-zone case based on the Högsjö Västra infrastructure project. The simulations showed that abrupt changes in support stiffness produce more pronounced local variations in sleeper forces, whereas more gradual stiffness transitions result in smoother load transfer. The application represents an initial step towards using the developed framework for performance-based assessment of railway transition zones.

Overall, DigiRail demonstrates that coupled DEM–FEM–MBD simulation can be applied to railway problems at increasingly realistic system scales and can reproduce important aspects of measured physical behaviour. The developed methods are particularly valuable where the interaction between granular materials, structures and machinery governs performance and where conventional calculation methods cannot resolve the underlying mechanisms. Continued development should focus on full-scale validation, improved determination of support stiffness, more detailed vehicle models, explicit ballast breakage and statistical treatment of granular variability. These developments provide a path towards integrating advanced physics-based simulation with established engineering methods for the design, construction and maintenance of future railway infrastructure.

Swedish version

DigiRail har utvecklat och validerat ett högpresterande numeriskt ramverk för fysikbaserad simulering av järnvägsinfrastruktur under byggnation, drift och underhåll. Projektet adresserar en central utmaning inom järnvägsteknik: spårsystemet består av komponenter med fundamentalt olika mekaniskt beteende, från granulär järnvägsmakadam och andra obundna material till räler, sliprar, underliggande konstruktioner, fordon samt bygg- och underhållsmaskiner. Samspelet mellan dessa delar är avgörande för bland annat sättningar, lastfördelning, kompaktering, nedbrytning av makadam och den dynamiska responsen i övergångszoner.

Det utvecklade ramverket kombinerar diskreta elementmetoden (DEM), finita elementmetoden (FEM) och fler-kroppsdynamik (MBD). DEM används för att beskriva makadam och andra grova granulära material på partikelnivå, FEM används för konstruktionsdelar och kontinuerliga materialdomäner, medan MBD ger en effektiv representation av fordon och maskiner. De numeriska metoderna kompletteras med automatiserade arbetsflöden för modellgenerering, kalibrering, hantering av simuleringsstudier och körning på högpresterande beräkningsresurser.

En kopplad DEM–FEM-modell av järnvägsspåret utvecklades som gemensam plattform för de järnvägsspecifika studierna. Arbetet omfattade kalibrering av makadamens mekaniska beteende, effektiv generering av stora makadambäddar, realistiska representationer av icke-sfäriska och icke-konvexa partiklar, behandling av randvillkor för ändliga spårmodeller, spårlägesfel samt dynamiska rörliga laster. Studierna visade att partikelrepresentationen har en tydlig påverkan på den beräknade spårresponsen. Icke-konvexa partiklar gav starkare geometrisk låsning, högre spårstyvhet och mindre sättning än motsvarande konvexa partikelrepresentationer.

Experimentell validering genomfördes på flera skalnivåer. Kopplade DEM–MBD-simuleringar av fullskalig vibrationspackning återgav den huvudsakliga utvecklingen av sättning under 14 vältöverfarter samt viktiga egenskaper hos det uppmätta marktrycket. Simuleringarna gjorde det dessutom möjligt att studera hur packningsgraden utvecklades med djupet i det granulära lagret, vilket är information som är svår att erhålla experimentellt.

Den generella DEM–MBD-metodiken för sam-simulering utvärderades även mot fullskaliga försök med hjullastare. Modellen återgav viktiga delar av skopfyllnad, deformation av materialhögen och maskinrespons för flera körsekvenser, medan andra fall tydliggjorde begränsningar i den förenklade maskinmodellen. Resultaten ger därmed både validering av kopplingsmetodiken och vägledning för fortsatt modellutveckling.

Järnvägsmakadamens beteende studerades genom storskaliga slipersförskjutningsförsök, cykliska ödometerförsök och motsvarande DEM-simuleringar. Resultaten visade att kornstorleksfördelningen påverkar deformation, styvhet och nedbrytning, medan inspänning och vertikal last har stor betydelse för den mobiliserade laterala resistansen. DEM-simuleringarna återgav de huvudsakliga relativa trenderna mellan de undersökta materialen och gav ytterligare information om partikelomlagring och kraftöverföring.

På konstruktionsnivå jämfördes DEM–FEM-simuleringar med mätningar från ett fullskaligt försök med en trågbro. Simuleringarna återgav den övergripande storleksordningen och den rumsliga fördelningen av trycket från makadambädden och visade att olika realiseringar av samma granulära bädd kan ge asymmetriska lokala lastmönster även vid nominellt symmetrisk belastning. Detta illustrerar betydelsen av makadamens diskreta och stokastiska struktur för lastöverföringen till underliggande konstruktioner.

Ett kopplat DEM–MBD-ramverk utvecklades även för järnvägsstoppning och kalibrerades mot driftsdata från en helhydraulisk stoppmaskin. De undersökta simuleringarna indikerar att maskinkoncept och manöverstrategi kan påverka både uppnådd packningsgrad och de krafter som enskilda makadampartiklar utsätts för. Arbetet visar potentialen i att använda detaljerad simulering för att samtidigt studera underhållseffektivitet och bevarande av makadamens kvalitet, samtidigt som ytterligare experimentell validering och explicit modellering av partikelnedbrytning är viktiga fortsatta utvecklingssteg.

Slutligen tillämpades järnvägsmodellen på en övergångszon baserad på infrastrukturprojektet Högsjö Västra. Simuleringarna visade att abrupta förändringar i undergrundens styvhet ger tydligare lokala variationer i sliperskrafterna, medan mer gradvisa styvhetsövergångar ger en jämnare lastöverföring. Tillämpningen utgör ett första steg mot att använda det utvecklade ramverket för funktionsbaserad analys av övergångszoner i järnvägsinfrastruktur.

Sammantaget visar DigiRail att kopplad DEM–FEM–MBD-simulering kan användas för järnvägsproblem på alltmer realistiska systemskalor och återge viktiga delar av det uppmätta fysikaliska beteendet. Metoderna är särskilt värdefulla i problem där samspelet mellan granulära material, konstruktioner och maskiner styr systemets respons och där konventionella beräkningsmetoder har begränsad möjlighet att beskriva de bakomliggande mekanismerna. Fortsatt utveckling bör fokusera på fullskalig validering, förbättrad bestämning av effektiv undergrundsstyvhet, mer detaljerade fordonsmodeller, explicit modellering av makadambrott samt statistisk behandling av naturlig variation i granulära material. Detta skapar en väg mot att kombinera avancerad fysikbaserad simulering med etablerade ingenjörsmetoder för projektering, byggnation och underhåll av framtidens järnvägsinfrastruktur.

Contents

1 Background and Project Objectives **1**

1.1 Background . . . 1

1.2 Project Objectives . . . 3

2 Overall Modelling Framework **4**

3 Modelling of Railway Rock Particles **5**

3.1 Numerical Railway Model . . . 5

3.2 Material Models and Calibration . . . 5

3.3 Ballast Bed Generation . . . 6

3.4 Particle Representation . . . 7

3.5 Railway Transition Zone Model . . . 7

3.6 FEM Boundary Elements . . . 8

3.7 Load Models . . . 9

3.7.1 Rail Irregularities . . . 9

3.7.2 Moving Mass Model . . . 10

3.8 Summary . . . 10

4 Validation of Machine and Vehicle MBD/DEM FMI Coupling **13**

4.1 Simulation and Validation of Vibratory Roller Compaction of Unbound Granular Materials . . . 13

4.1.1 Background and Objectives . . . 13

4.1.2 Coupled DEM–MBD Simulation Framework . . . 13

4.1.3 Numerical results and validation . . . 15

4.1.4 Discussion and future work . . . 18

4.2 Validation of Coupled DEM–MBD Wheel Loader Simulations against Full-Scale Loading Experiments . . . 18

4.2.1 Virtual product development . . . 18

4.2.2 Experiment setup . . . 19

4.2.3 Simulation setup . . . 20

4.2.4 Validation . . . 21

4.2.5 Conclusions . . . 22

5 Validation of Railway Structure Models under Operational Load Cases **26**
5.1 Experimental Validation of Ballast Behaviour and DEM Modelling 26
5.1.1 Sleeper Push Tests and DEM Simulations 26
5.1.2 Cyclic Oedometer Tests and DEM Simulations 27
5.1.3 Conclusions and Future Work 29
5.2 DEM-FEM Simulations of a Trough Bridge 30
5.2.1 Method 30
5.2.2 Results 31
5.2.3 Discussion and Conclusion 32

6 Validation and Investigation of Critical Maintenance Operations **34**
6.1 Background 34
6.2 Development of the Co-Simulation Framework 34
6.3 Model Calibration 35
6.4 Results 36
6.5 Conclusions 38

7 Investigation of Transition Zones and Verification against Analytical Calculation Methods **39**
7.1 Application of the Transition Zone Model to Högsjö Västra 39
7.1.1 Simulation Model 39
7.1.2 Results 41
7.1.3 Limitations and future development 42

8 Conclusions and Recommendations **43**
8.1 Conclusions 43
8.2 Recommendations 44

References **46**

1. Background and Project Objectives

1.1. Background

Railway infrastructure is a central component of a sustainable and reliable transport system. In Sweden, the railway network is also of strategic importance for industry and freight transport, with the Iron Ore Line being a particularly important example. At the same time, there is a continuing need to maintain the condition and extend the service life of existing infrastructure while developing new infrastructure capable of meeting future requirements on capacity, axle loads, availability and environmental performance [1–3].

A ballasted railway track is a mechanically complex system consisting of components with fundamentally different material behaviour and characteristic length scales. Dynamic loads from passing vehicles are transferred from the rail and sleepers through the granular ballast and underlying unbound layers to the embankment and subgrade. The resulting structural response depends on the interaction between vehicle loading, track geometry, structural stiffness, granular material behaviour and the mechanical properties of the supporting ground. Repeated loading can result in particle rearrangement, settlement and degradation of the ballast, which in turn influence track geometry and stiffness over time [4–7].

The interaction between the individual parts of the track structure becomes particularly important at locations where the mechanical properties change over relatively short distances. Transition zones between conventional ballasted track and bridges, culverts or other comparatively stiff structures are prominent examples. Abrupt changes in vertical track stiffness can alter the dynamic interaction between vehicle and track and contribute to differential settlement and increased maintenance demand [8, 9]. Similar system-level interactions are important when evaluating changes in axle load, modifications to the supporting layers, under-sleeper pads or changes in the mechanical properties of the substructure.

These challenges create a need for calculation methods that can represent the railway infrastructure as an interacting system and predict how changes in material properties, geometry, loading and structural design affect its mechanical performance. Such predictive capabilities are also relevant in the transition from predominantly prescriptive technical requirements towards functional and performance-based requirements for structures, components and construction materials. Rather than specifying only how a railway structure should be constructed, a performance-based approach increasingly requires the ability to evaluate whether a proposed solution provides the required stiffness, load distribution, deformation behaviour and long-term functionality.

Numerical simulation provides an important tool for this type of analysis. However, no single conventional numerical method is naturally suited to all components of a ballasted railway system. Continuum-based methods such as the Finite Element Method (FEM) are well established for modelling structural components, soil and embankment materials. Railway ballast, on the other hand, is a granular material whose behaviour is governed by the movement, rotation and contact interaction of individual particles. The Discrete Element Method (DEM) provides a natural framework for representing these mechanisms and has consequently become an established research method for studying railway ballast, including settlement, particle degradation and ballast–sleeper interaction [4, 7, 10, 11].

DEM also makes it possible to explicitly account for particle size and shape. These properties have a significant influence on the mechanical response of coarse granular materials and railway ballast, and several approaches for representing realistic non-spherical particles have been developed [12, 13]. For engineering-scale applications, however, a detailed particle representation results in considerable computational demands. High-performance implementations using graphics processing units (GPUs) therefore provide an important enabling technology for extending particle-resolved simulations from laboratory specimens towards larger infrastructure systems [14, 15].

A system-level railway model consequently benefits from combining different numerical descriptions. FEM can be used for structural components and supporting continuum layers, DEM for ballast and other coarse unbound materials, while Multi-Body Dynamics (MBD) provides an efficient representation of vehicles and construction or maintenance machinery. Coupled DEM–FEM approaches have previously demonstrated the potential to resolve interactions between ballast and structural components [16, 17], while coupled DEM–MBD methods provide corresponding possibilities for machinery and maintenance operations such as tamping [18]. Bringing these descriptions together within a computationally efficient framework creates the possibility of studying mechanisms that are difficult to capture when the individual parts of the railway system are analysed separately.

This system perspective is relevant throughout the railway life cycle. During construction, material handling and compaction influence the density, stiffness and spatial variability of embankment and granular layers [19]. During operation, train loads interact with the complete track structure and can generate accumulated settlement and ballast degradation, particularly at locations with changes in structural stiffness [6, 9]. During maintenance, operations such as tamping intentionally rearrange the ballast to restore track geometry and support, but may simultaneously contribute to particle degradation and changes in the ballast structure [18]. A common modelling framework capable of representing these different stages provides opportunities to connect construction quality, operational performance and maintenance requirements within the same mechanical description.

The technical foundation for DigiRail originated from the preceding InfraSweden2030 project DigiRoad. Within DigiRoad, high-performance DEM methods were developed for large-scale simulation of unbound rock materials and their interaction with construction machinery. The work included GPU-accelerated simulation of realistic non-spherical particles and coupling between DEM and models of construction equipment. Building on these capabilities, the DigiRail project was initiated in 2022 within the Vinnova-funded strategic innovation programme InfraSweden2030, with the objective of extending the modelling framework from road construction to railway infrastructure. A central development was the coupling between DEM and FEM, complemented by existing capabilities for coupling DEM with MBD.

The DigiRail consortium brought together Fraunhofer-Chalmers Centre (FCC), NCC, Dynapac Compaction Equipment, Volvo Construction Equipment, Infranord, Ramboll and Trafikverket. The consortium was formed to represent several parts of the railway life cycle, including construction materials, construction machinery, infrastructure construction, engineering design and railway maintenance. This provided both application cases and experimental environments for development and validation of the numerical methods.

A complementary research activity was subsequently established with funding from Trafikverket's FoI portfolio *Bygga*. The Trafikverket-supported activities retained the common DigiRail framework but increased the emphasis on railway-specific validation, track stiffness, ballast–structure interaction and transition zones. They also strengthened the connection between the developed simulation methods and conventional engineering analysis, with particular interest in the future use of physics-based simulation as support for functional and performance-based design of railway infrastructure.

The combined DigiRail programme therefore addressed both a numerical and an engineering challenge: to develop sufficiently detailed and computationally efficient models of the interacting railway system, and to establish through verification and experimental validation whether these models can provide useful predictions at scales relevant to engineering

applications.

1.2. Project Objectives

The overall objective of DigiRail was to **develop and validate a high-performance coupled numerical framework for physics-based simulation of railway infrastructure across relevant system scales**, integrating the Discrete Element Method (DEM), Finite Element Method (FEM) and Multi-Body Dynamics (MBD).

The framework was intended to enable the railway infrastructure to be analysed as an interacting mechanical system rather than as a collection of isolated components. Depending on the application, the model could include the soil and embankment, unbound aggregate layers, railway ballast, sleepers, rails, vehicles and machinery used during construction and maintenance.

More specifically, the project had the following technical and application-oriented objectives:

1. **Develop a robust and computationally efficient coupled DEM–FEM–MBD methodology** suitable for railway infrastructure simulations at engineering-relevant scales.
2. **Establish appropriate material and component models** for the principal parts of the railway system, including realistic particle-based representations of ballast and unbound rock materials together with FEM representations of structural and supporting layers.
3. **Verify and validate the numerical models against experimental data** using a hierarchy of material tests, component-scale experiments and full-scale validation cases.
4. **Demonstrate the modelling framework for different stages of the railway life cycle**, including construction, operational train loading and maintenance.
5. **Investigate applications in which interactions between granular materials, structures, vehicles and machinery are particularly important**, including vibratory compaction, ballast–sleeper interaction, ballast–bridge interaction, track transition zones and tamping operations.
6. **Evaluate the potential of detailed physics-based simulation as support for performance-based railway engineering**, including analysis of track stiffness, load distribution and transition zones, and comparison with established analytical or conventional numerical engineering methods.
7. **Make the developed methods accessible to the project consortium through a software demonstrator and application-specific simulation models**, enabling industrial evaluation, knowledge transfer and subsequent development beyond the project.

Validation was a central part of the project methodology. The objective was not only to demonstrate that increasingly large and detailed railway systems could be simulated, but to determine whether the calculated response reproduced measurable physical behaviour with sufficient accuracy for the intended application. Model development, experimental investigation and application studies were therefore carried out iteratively throughout the work packages.

The original Vinnova-funded project and the complementary Trafikverket activities shared the same overall technical framework but placed somewhat different emphasis on its application. The original InfraSweden2030 project established the general multi-physics framework and addressed applications across construction, operation and maintenance. The Trafikverket-funded activities provided additional focus on railway infrastructure validation, transition zones, track stiffness and the connection between detailed numerical simulation and engineering calculation methods. The present report therefore treats the two funding activities as parts of one continuous DigiRail research and development programme.

2. Overall Modelling Framework

The DigiRail modelling framework was developed as a modular environment for analysing railway infrastructure as an interacting mechanical system. Different numerical descriptions are used where they are most appropriate: the Discrete Element Method (DEM) resolves ballast and other coarse unbound materials at particle scale, the Finite Element Method (FEM) represents rails, sleepers, structures and supporting continua, and Multi-Body Dynamics (MBD) represents vehicles and construction or maintenance machinery. Coupling between these domains enables forces, motions and structural response to be transferred during the simulation.

As illustrated in Figure 2.1, the numerical models are supported by a common computational workflow. During the project, tools were developed for automated model and geometry generation, calibration and validation against experimental data, parameter studies, high-performance computing (HPC) execution and simulation management. Railway-specific capabilities, including dynamic moving loads, rail irregularities and FEM boundary extensions, were integrated into the same framework. This modular structure makes it possible to reuse the underlying methods across different applications while adapting the physical model to the problem being studied.

The resulting platform provides the computational basis for the subsequent investigations in DigiRail. The same core methodology is used for construction processes such as vibratory compaction, operational railway problems including ballast–structure interaction and transition zones, and maintenance operations such as tamping. In this way, the project connects detailed material behaviour with system-level infrastructure and machine response within a common simulation framework.

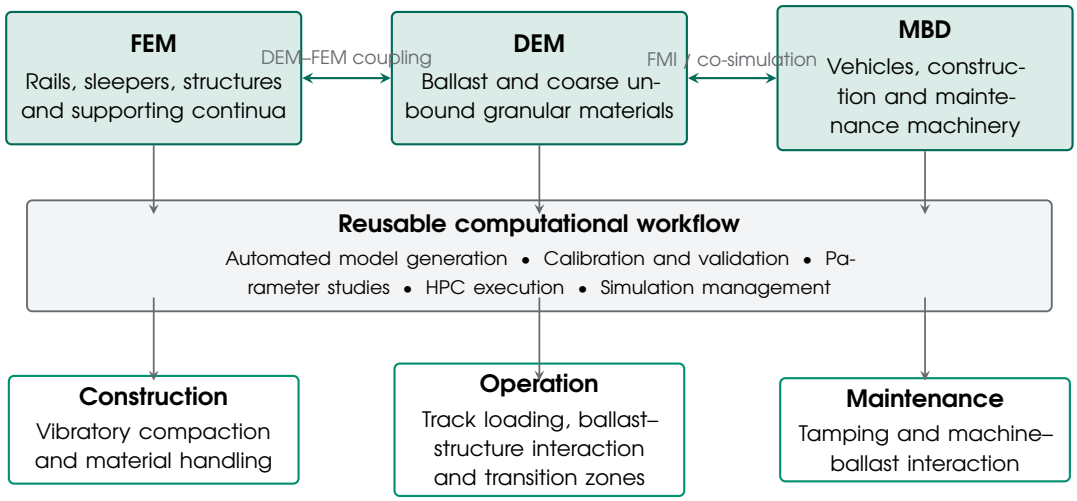


Figure 2.1. Overview of the DigiRail modelling framework. DEM, FEM and MBD provide complementary descriptions of granular materials, railway structures, vehicles and machinery. A common computational workflow supports model generation, calibration, validation and high-performance simulation across construction, operation and maintenance applications.

3. Modelling of Railway Rock Particles

3.1. Numerical Railway Model

To investigate the mechanical behaviour of railway infrastructure under operational loading, a numerical model capable of resolving both the structural response of the track and the discrete behaviour of the ballast is required. Conventional continuum approaches cannot explicitly capture ballast particle interactions, while purely discrete models become computationally expensive for large railway systems. Therefore, a coupled DEM-FEM approach was adopted to combine the strengths of both modelling techniques.

Within DigiRail, a coupled DEM-FEM model representing a railway track was developed and continuously extended throughout the project. The rails, sleepers and supporting structures were represented using finite elements, while the ballast layer was modelled using the discrete element method. A surface coupling between both domains enables the transfer of forces and displacements and motions during the simulation, allowing the interaction between ballast particles and the structural components to be captured. The modelling framework is sufficiently flexible to represent different railway configurations, including conventional track sections of varying lengths and transition zones. Model generation routines were developed to efficiently create these baseline configurations for subsequent investigations.

The resulting framework enables simulation of complete railway track segments under static and dynamic loading while explicitly accounting for ballast particle behaviour. It forms the basis for all subsequent investigations presented in this report, including material calibration, particle shape studies, transition zone analyses and application for industrial use-cases.

The developed DEM-FEM railway model provides a common simulation platform that allows different modelling assumptions and numerical developments to be evaluated within a consistent framework. This significantly improves the comparability of individual studies and provides the foundation for further development.

3.2. Material Models and Calibration

Railway infrastructure consists of components made from materials with fundamentally different mechanical behaviour, ranging from steel rails and concrete sleepers to granular railway ballast. To obtain a realistic representation of the track, appropriate material models and parameters are therefore required for both the continuum and discrete domains.

Within the DEM-FEM framework, the rails, sleepers and supporting structures were modelled as linear elastic materials. Material properties were selected from published literature and, where available, based on the materials used in the trough bridge experiments performed at LTU [20]. The interaction between rails and sleepers was represented using a penalty-based contact formulation.

Since the behaviour of DEM simulations is highly dependent on the selected particle and contact parameters, the ballast material was calibrated prior to the railway simulations. The calibration was performed by reproducing the direct shear experiments reported by Jia et al. [21]. In Figure 3.1 an illustration of the experimental rig and a snapshot of the corresponding

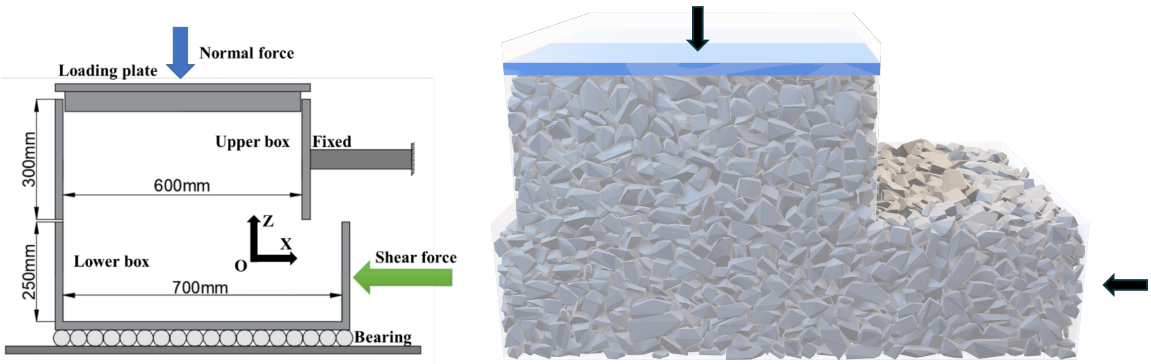


Figure 3.1. The illustration of the experimental test rig as by [21] (left) and the corresponding DEM realisation (right).

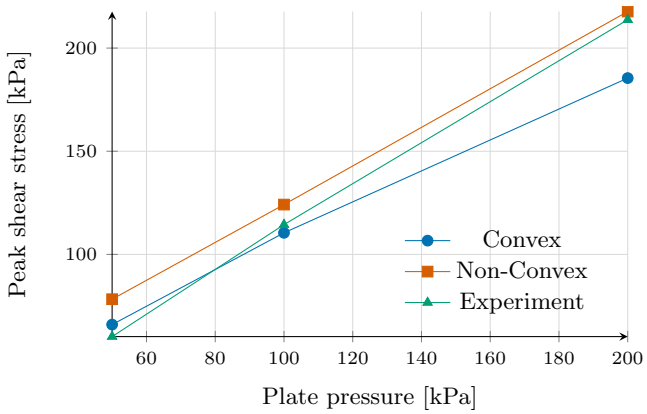


Figure 3.2. Comparison of Mohr diagram: published experiment by Jia et al. [21], the calibrated DEM simulation with convex particles, and the DEM simulation with calibrated parameters with non-convex particles.

DEM simulation are shown. The objective was to reproduce both the measured peak shear stresses and the inclination of the resulting Mohr-Coulomb failure envelope. The calibration of the DEM simulation was performed for a convex particle representation. Building up on this, the calibrated parameters have also been applied to a non-convex particle representation for the comparison shown in Figure 3.2.

The calibrated parameter set showed good agreement with the experimental results for recycled railway ballast, providing confidence that the DEM model adequately reproduces the macroscopic shear behaviour required for the subsequent railway simulations.

While this calibration was performed using convex dilated polyhedra, railway ballast particles are naturally non-convex. Additionally, the simulations of the direct shear test with non-convex particles yield a better match for the highest pressure level. This raises the question of whether explicitly representing particle non-convexity influences the mechanical response of railway tracks. This question is investigated in section 3.4.

3.3. Ballast Bed Generation

The preparation of large DEM particle populations is computationally demanding. To enable efficient and reproducible railway simulations, a preparation workflow was developed that separates the computationally expensive initialization from the subsequent loading simulations. As a result, the ballast preparation only needs to be performed once for a given track configuration and can subsequently be reused for multiple simulation scenarios.

The developed preparation routine consists of

1. The generation of a unit cell filled with railway ballast particles with a temporarily reduced inter-particle friction to obtain the desired packing density.
2. The complete ballast bed volume is filled based on periodic cell replication [22].
3. The sleepers and rails are introduced in the simulation and settle under gravity onto the ballast bed, while more particles are generated to fill the spaces between the sleepers.

The resulting preparation workflow provides a reproducible initial state for DEM-FEM railway simulations and substantially reduces the computational effort associated with repeated simulation studies, parameter investigations and validation analyses.

3.4. Particle Representation

Railway ballast particles exhibit highly angular and non-convex geometries, which strongly influence their mechanical behaviour through geometric interlocking. While spherical particles are computationally efficient, they cannot adequately reproduce this behaviour. Fully resolved polyhedral particles provide a more realistic representation but are associated with a substantially higher computational cost. An efficient particle representation is therefore required that balances computational efficiency and modelling accuracy.

Within the DEM-FEM framework, ballast particles were represented using the dilated polyhedral model available in Demify. This representation captures particle angularity while remaining computationally efficient compared to fully resolved polyhedral geometries. Furthermore, Demify allows particles to be represented as compound shapes consisting of multiple convex dilated polyhedra, enabling the preservation of particle non-convexity without the computational expense of fully resolved non-convex particles. To investigate the influence of particle shape on railway track behaviour, a dedicated study comparing convex and non-convex particle representations was performed using the developed DEM-FEM railway model under both static and dynamic loading conditions. A preprint of the research article is available while it is under review: [23].

The non-convex particle representation consistently resulted in reduced settlement accumulation, increased coordination numbers and higher vertical track stiffness compared with the convex representation. In addition, a substantially larger proportion of particles exhibited low rotational activity, indicating enhanced geometric interlocking within the ballast layer. These observations demonstrate that the additional geometric complexity primarily affects the stability of the ballast layer by restricting particle rotations and improving force transmission.

The study demonstrates that particle shape has a significant influence on ballast behaviour at the track scale. Incorporating particle non-convexity therefore improves the realism of DEM railway simulations and should be considered when investigating settlement, track stiffness and long-term ballast performance.

3.5. Railway Transition Zone Model

Railway transition zones, such as the transition between an embankment and a bridge, are characterized by abrupt changes in support stiffness. These stiffness contrasts can lead to differential settlement and increased dynamic loading of the track. A numerical model capable of representing variations in support conditions is therefore required to investigate the mechanical behaviour of railway transition zones.

Within the developed DEM-FEM framework, the rails and sleepers are represented using their actual geometries. In addition, routines were developed to facilitate the modelling of detailed railway geometries, including the embankment geometry shown in Figure 3.3, which represents a section of the planned Västlänken railway track in Gothenburg[1]. While

[1]More information about Västlänken is available at https://www.trafikverket.se/vara-projekt/projekt-i-vastra-gotalands-lan/vastlanken/

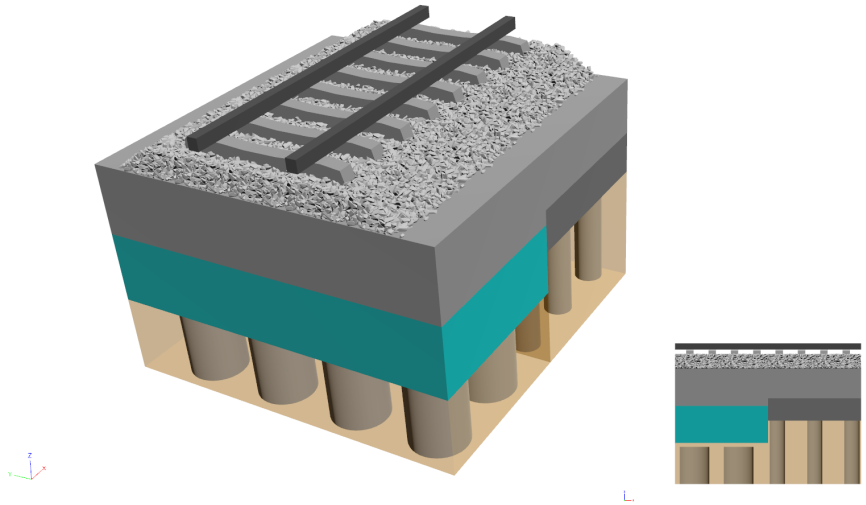


Figure 3.3. Simulation model of a railway track segment with detailed embankment geometry based on a section of the planned Västlänken railway track.

such detailed geometries provide a realistic representation of the railway structure, obtaining and processing the required geometrical data can be challenging. Furthermore, explicitly modelling large volumes of soil and embankment material increases the computational cost of the simulations.

To enable efficient investigation of different transition zone configurations, the supporting structure beneath the ballast layer can therefore be idealised as a spatially varying elastic foundation, as shown in Figure 3.4. Rather than explicitly modelling the complete bridge and embankment geometry, the support stiffness is varied longitudinally along the track to represent the governing stiffness transition between different support conditions, for instance, between a soil-supported track and a concrete bridge. The stiffness variation can be defined using different characteristic functions, allowing different transition zone designs to be investigated within the same modelling framework.

This idealisation captures the dominant stiffness variation governing the track response while avoiding the computational expense associated with explicitly modelling large soil and embankment volumes. It therefore provides a flexible and computationally efficient approach for systematically investigating the influence of different support-stiffness transitions on railway track behaviour.

3.6. FEM Boundary Elements

Since the model represents only a finite section of railway track, the influence of the rail boundaries on the simulated response was investigated. The study showed that the boundary effects are significant and influence the load transfer along the transition zone. Stable results were only obtained from approximately the sixth sleeper measured from the track ends, demonstrating that the boundary treatment must be considered when analyzing transition zone behaviour. Conventional periodic boundary conditions cannot be applied to transition zones because the different support stiffnesses result in non-periodic rail displacements and differential settlement.

To overcome this limitation, FEM boundary elements were developed and incorporated into the DEM-FEM coupling framework, as shown in Figure 3.5. A summary of simulation results is given in Figure 3.6, where the forces acting on the individual sleepers as well as their settlement are visualised for a single load traversing the track. The figures in the top row show the results without FEM boundary elements and the bottom row with the FEM boundary elements. The results indicate that the high peaks in both force and settlement at the domain boundary smoothen and decrease when introducing the boundary elements, showing

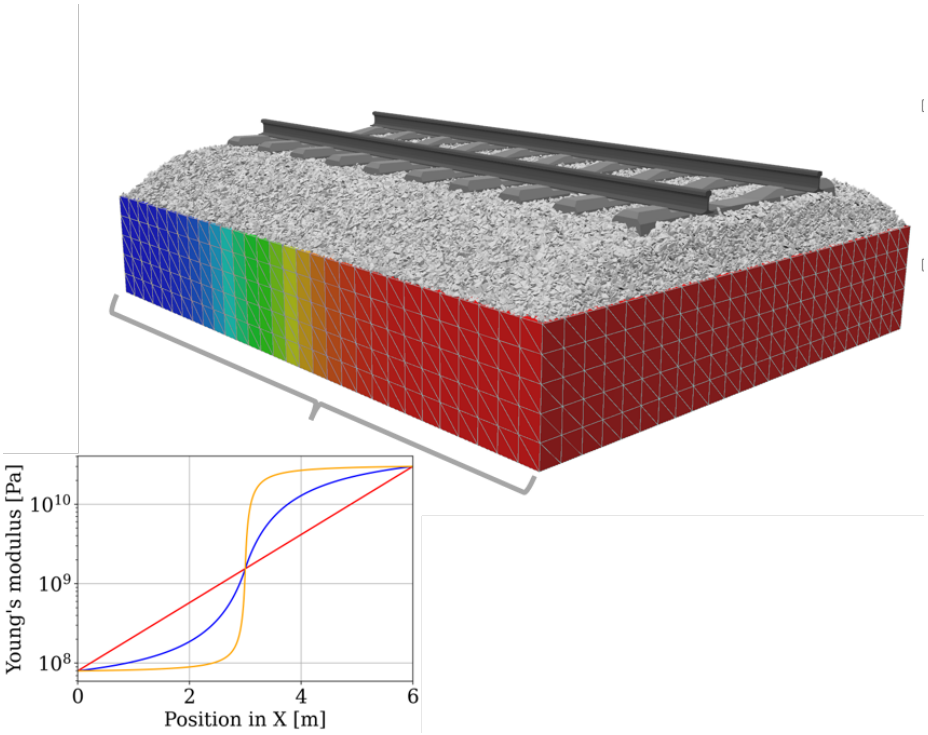


Figure 3.4. Idealised simulation model of a railway transition zone. The support stiffness varies longitudinally along the track and can be adjusted to represent different transition-zone configurations.

more stable and consistent results across the track. Thus, the FEM boundary elements reduce artificial boundary effects and enable realistic simulation of finite transition zones.

The developed transition-zone model provides an efficient representation of stiffness transitions while maintaining the computational efficiency required for large-scale DEM-FEM simulations. Together with the FEM boundary elements, it enables realistic investigation of load transfer and settlement behaviour in railway transition zones.

3.7. Load Models

Real railway traffic does not apply a constant force to the track. Instead, the wheel loads are influenced by vehicle dynamics and rail irregularities, resulting in spatially varying contact forces. To improve the realism of the DEM-FEM railway simulations, the loading model was therefore extended beyond conventional stationary and moving load approaches.

3.7.1. Rail Irregularities

As a first step, a stochastic rail irregularity model based on the formulation proposed by Podwórna [24] was implemented. The model generates realistic rail profiles from a power spectral density function and enables dynamic excitation of the railway track due to surface imperfections.

To obtain representative conditions for Swedish railway infrastructure, the model parameters were adjusted using rail irregularity measurements provided by Trafikverket from the Högsjö test site. Although additional measurement data would be required to establish characteristic irregularity spectra for Swedish railways, the available dataset provided a suitable basis for an initial calibration. Figure 3.7 provides a comparison of the measurement data and the modelled irregularity results.

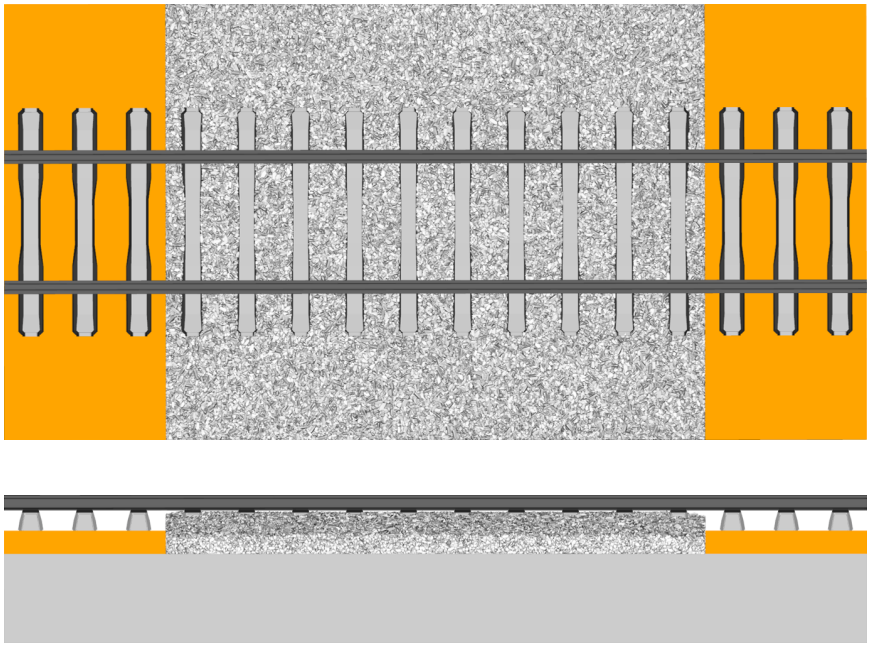


Figure 3.5. Visualisation of the extended railway track with FEM boundary elements for the railway ballast (highlighted in orange).
Top: Top view of the extended railway track.
Bottom: Side view of the extended railway track.

3.7.2. Moving Mass Model

Conventional moving load models prescribe the axle load independently of the structural response of the track. Consequently, they cannot represent the interaction between the vehicle and the railway infrastructure. To address this limitation, a moving mass model was developed within the DEM-FEM framework.

The implemented model represents the bogie by a single-degree-of-freedom spring-damper system travelling along the rails. The wheel force is continuously updated according to the relative motion between the vehicle and the rail, allowing the axle load to respond to rail irregularities and track deformations.

As an initial verification, the moving mass model was evaluated using representative vehicle parameters obtained from the literature. The results of the vertical position, velocity and forces of the moving mass based on a set of irregularities is shown in Figure 3.8. The simulations demonstrate that the model produces dynamically varying wheel forces in response to the generated rail irregularities, illustrating the expected interaction between the vehicle mass and the track.

The developed loading model extends the capabilities of the DEM-FEM railway framework by enabling more realistic representation of vehicle-track interaction than conventional moving load approaches. This provides the foundation for future investigations of dynamic railway behaviour, transition zones and differential settlement under operational loading.

3.8. Summary

Within AP3, a comprehensive DEM-FEM modelling framework for railway infrastructure was developed. The work included validated material models, efficient procedures for ballast bed generation, investigations of particle representation, the development of a simplified transition-zone model, and improved dynamic loading capabilities. Together, these developments provide a robust and computationally efficient simulation platform that forms the basis further validation studies and industrial use-cases presented in the subsequent work packages.

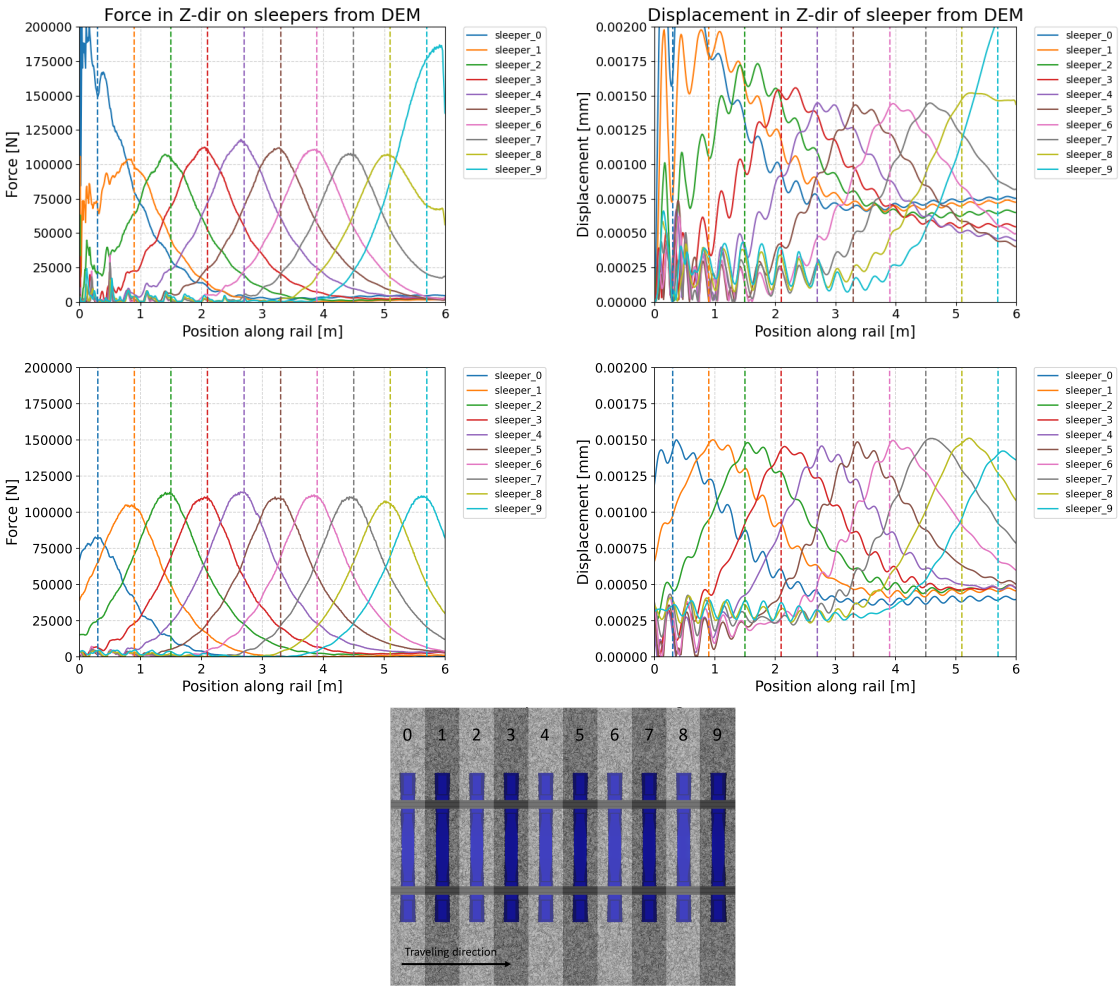


Figure 3.6. Demonstration on the simulation results of the FEM boundary elements: The force acting on (left) and the displacement of (left) each sleeper are shown for the simulations without (top) and with (bottom) FEM boundary elements. The sleeper IDs follow the labels shown at the bottom in the top view of the track.

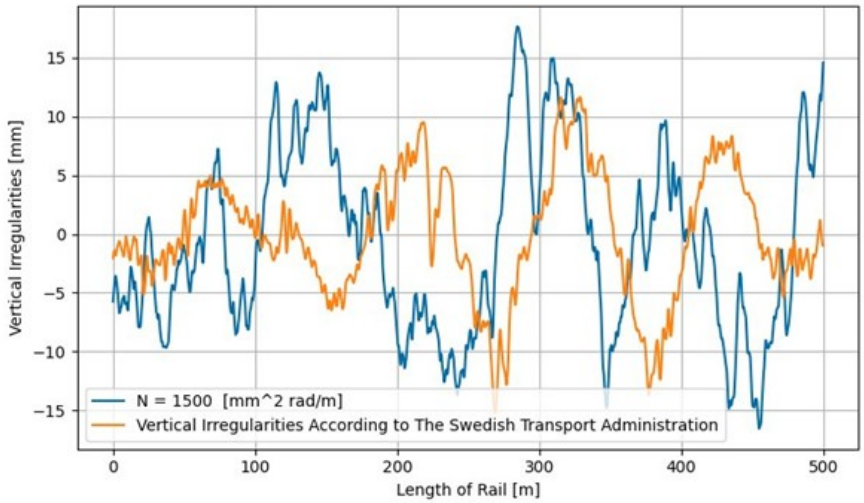


Figure 3.7. Visualisation of the provided rail irregularity measurements provided by Trafikverket (orange) and results of the implemented rail irregularity model adjusted to the measurement data (blue).

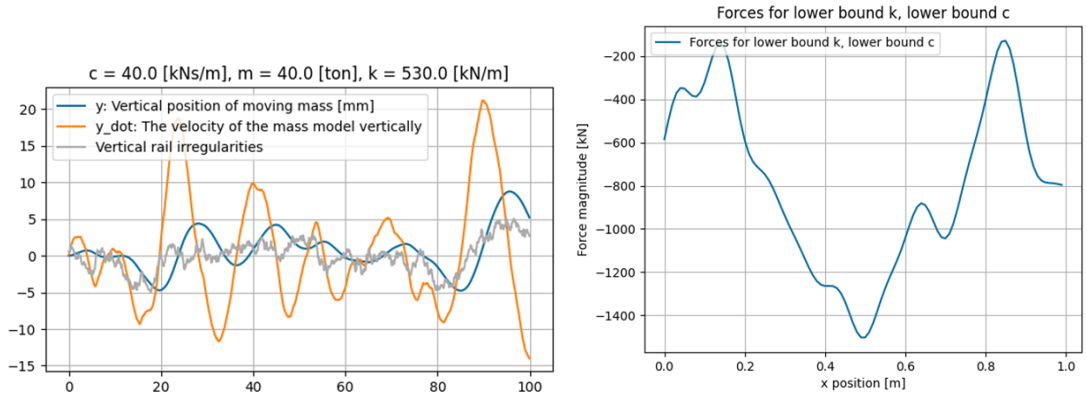


Figure 3.8. Simulation results of the moving mass model, including the vertical position (blue), the vertical velocity (orange), and the force magnitude (right figure), for a set of vertical rail irregularities (gray).

In addition to establishing the modelling framework, the work package generated important insights into the influence of modelling assumptions on railway simulations. The studies presented in this chapter demonstrate the importance of particle representation and appropriate boundary treatment for realistic prediction of railway track behaviour, thereby increasing the reliability of future DEM-FEM analyses.

4. Validation of Machine and Vehicle MBD/DEM FMI Coupling

4.1. Simulation and Validation of Vibratory Roller Compaction of Unbound Granular Materials

4.1.1. Background and Objectives

Compaction of unbound granular materials is an important process in the construction of roads, railways and other infrastructure systems. The final density and stiffness of the compacted layer strongly influence its long-term performance, while the efficiency of the compaction process affects both construction cost and environmental impact.

Within DigiRail WP4.1, a coupled numerical framework was therefore developed to simulate vibratory roller compaction of coarse unbound aggregates. The objective was to establish a validated simulation model capable of representing the interaction between the roller and the granular material, thereby creating a digital tool for analyzing compaction processes and supporting the development of intelligent compaction methods.

The work combined large-scale experimental data from the SBUF project 13820 with detailed DEM-MBD simulations. A comprehensive description of the experimental campaign, test procedures and measurements is available in the SBUF project report [25].

4.1.2. Coupled DEM–MBD Simulation Framework

The numerical framework combines the Discrete Element Method (DEM) and Multibody Dynamics (MBD) through a two-way coupling approach. The granular material is represented using DEM, allowing the motion and interaction of individual particles to be resolved explicitly. The vibration roller is represented by a multibody model that includes the drum, frame, eccentric shaft and suspension system. A overview of the simulation setup is show in Figure 4.1.

Following the experimental campaign, a total of 14 roller passes were simulated. This resulted in a comprehensive dataset describing the evolution of the granular bed throughout the compaction process. For each pass, several performance metrics were recorded, including ground pressure, bed settlement, packing density, and dynamic response data from the vibratory roller.

DEM model of the granular material

The granular material was represented using irregular, convex, dilation polyhedral particle shapes derived from scanned rock geometries, see Figure 4.2. The total domain size of the model was 5 m long, 2.5 m wide, and 1 m deep. The particle size distribution was obtained from experimental measurement of a material with a size distribution between +8/-90 mm. However, due to computational constraints, a slightly coarser particle distribution was used with particle size between +16/-90 mm.

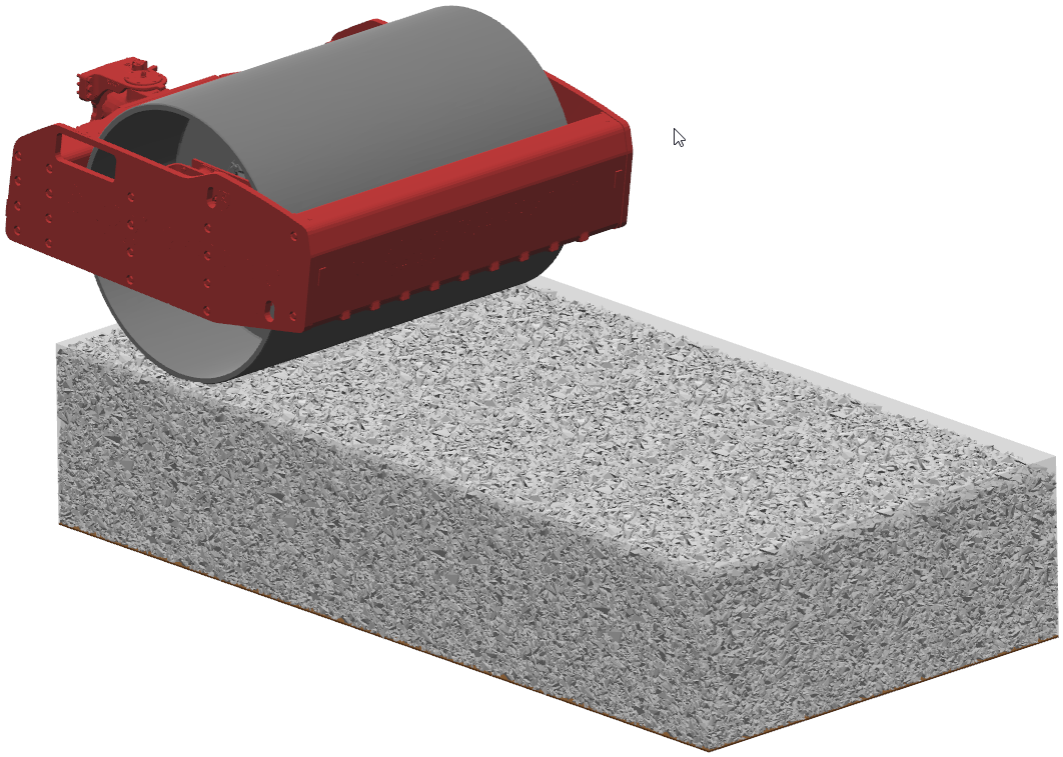


Figure 4.1. Overview of the compaction simulation model. In the figure one can see the granular bed modeled with DEM particles and the multibody model of the vibration roller.

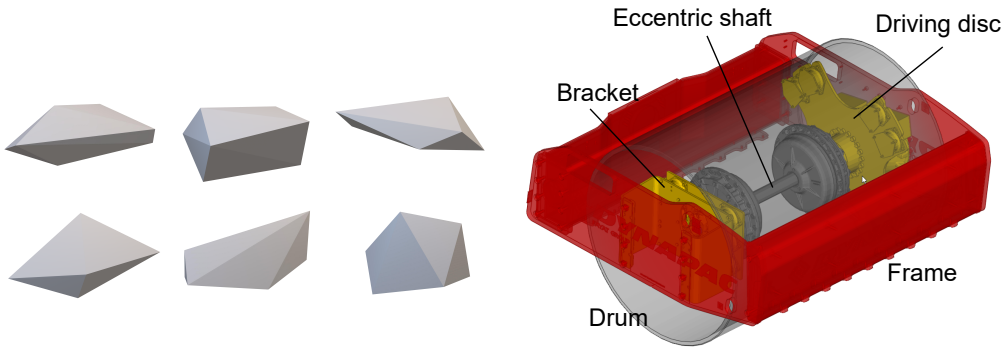


Figure 4.2. Left image: Illustration of the 6 rocks shapes used in the DEM model. Right Image: Overview of the different parts included in the MBD model.

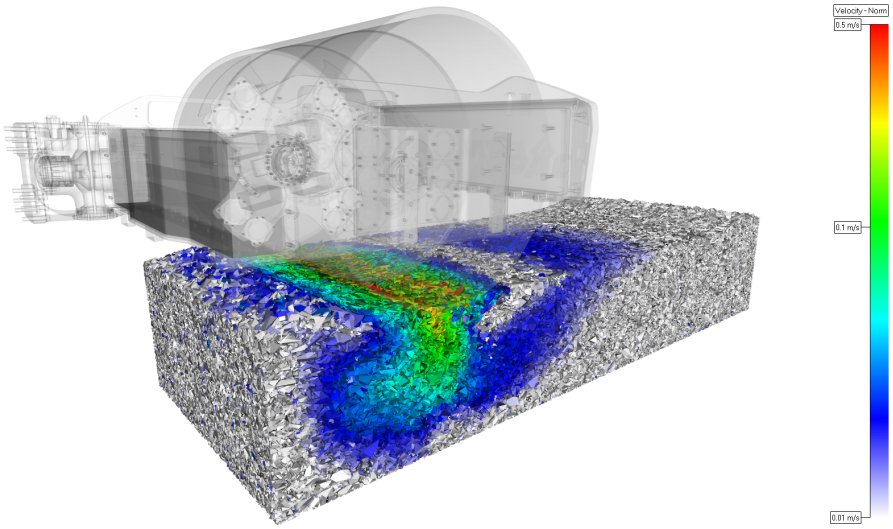


Figure 4.3. Overview of the velocity field in the particles during the third pass.

MBD model of the vibration roller

The roller model was based on a Dynapac CA3500D vibratory roller and included both low- and high-amplitude vibration settings. In the physical roller, these vibration settings are controlled by an eccentric shaft located inside the drum. To replicate this behavior, the MBD model explicitly represents the main components governing the roller dynamics, including the drum, frame, eccentric shaft, and suspension system. The vibration frequency is controlled through the rotational speed of the eccentric shaft, while the vibration amplitude is adjusted by varying the position of its center of gravity. This enables the numerical model to reproduce the frequency and amplitude settings used in the experimental campaign.

DEM-MBD coupling

The DEM model was implemented using the commercial solver Demify, while the vibratory roller was modelled using the open-source multibody dynamics solver EXUDYN. Since the granular material and the roller are represented in separate solvers, a coupling strategy is required to enable interaction between the two systems. In this work, a staggered co-simulation approach was adopted. At each time step, the DEM solver is first advanced and the contact forces acting between the granular material and the roller drum are evaluated. These forces, together with the corresponding contact moments, are then transferred to the MBD model and applied as external loads on the roller. The MBD solver is subsequently advanced one time step, after which the updated linear and angular velocities of the roller are extracted. These velocities are then imposed on the roller geometry in the DEM model, allowing the granular material to respond to the updated roller motion.

4.1.3. Numerical results and validation

To evaluate the predictive capability of the modeling framework, simulations were compared with measurements from the SBUF experimental campaign. As previously mentioned, 14 passes of the roller where simulated, and compared with the 14 passes performed in the experiments. The validation focused on quantities that are directly relevant for compaction performance, including settlement, packing density.

An illustration of the roller during the third pass is shown In Figure 4.3. The figure shows the velocity in each particle, where one can see pressure waves traveling through the bed.

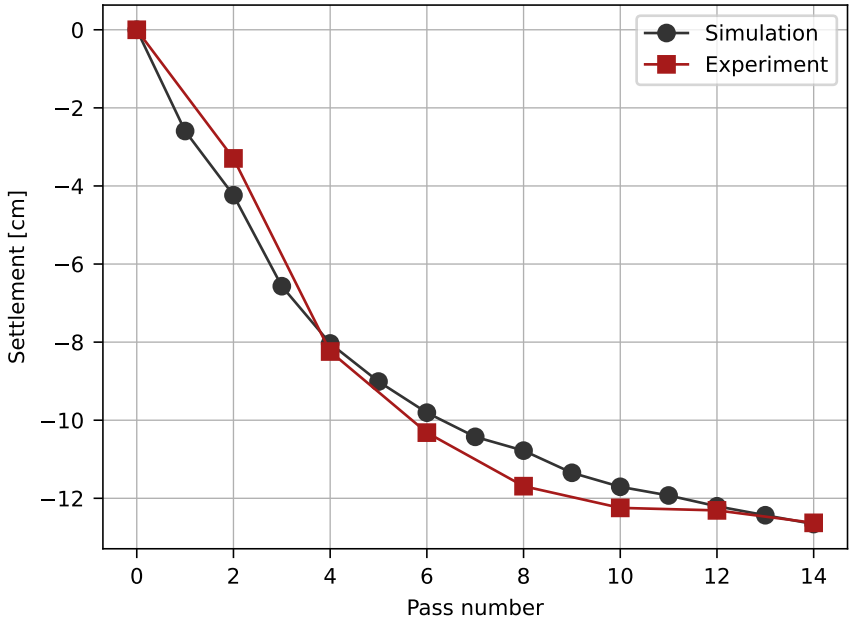


Figure 4.4. The bed settlement after each pass.

Settlement

The settlement after each pass is presented in Figure 4.4. In general, good agreement was obtained for the accumulated settlement of the granular layer during successive roller passes. Both simulations and experiments showed rapid deformation during the initial passes followed by a gradual reduction in settlement as the material approached a denser state.

Ground pressure

The ground-pressure measurements from the experiments and the simulations are compared in Figure 4.5. In both cases, the pressure was recorded using sensors installed at the bottom of the granular bed, enabling continuous measurement of the pressure response as the roller passed overhead.

Overall, the simulated pressure response shows good agreement with the experimental measurements. The model reproduces both the magnitude and the width of the pressure signal, as well as the temporal evolution of the pressure pulses generated by the vibratory roller. However, some discrepancies remain. In particular, the numerical model is unable to reproduce the gradual build-up of residual stresses observed in the experiments. As a result, the pressure level remaining in the bed after each pass is generally lower in the simulations than in the experimental measurements.

Packing density

The simulation framework has the unique capability, unlike the experiments, to investigate the evolution of packing density throughout the depth of the granular bed. Obtaining similar information experimentally would be challenging and would require intrusive measurement techniques.

Figure **??** presents the packing density as a function of bed depth for each compaction pass. The packing density is evaluated by sweeping a control volume of dimensions $3 \times 1 \times 0.2$ m through the center of the domain from the bottom of the bed to its surface. For each position, the packing density is computed as the ratio between the volume occupied by particles and the total volume of the control volume.

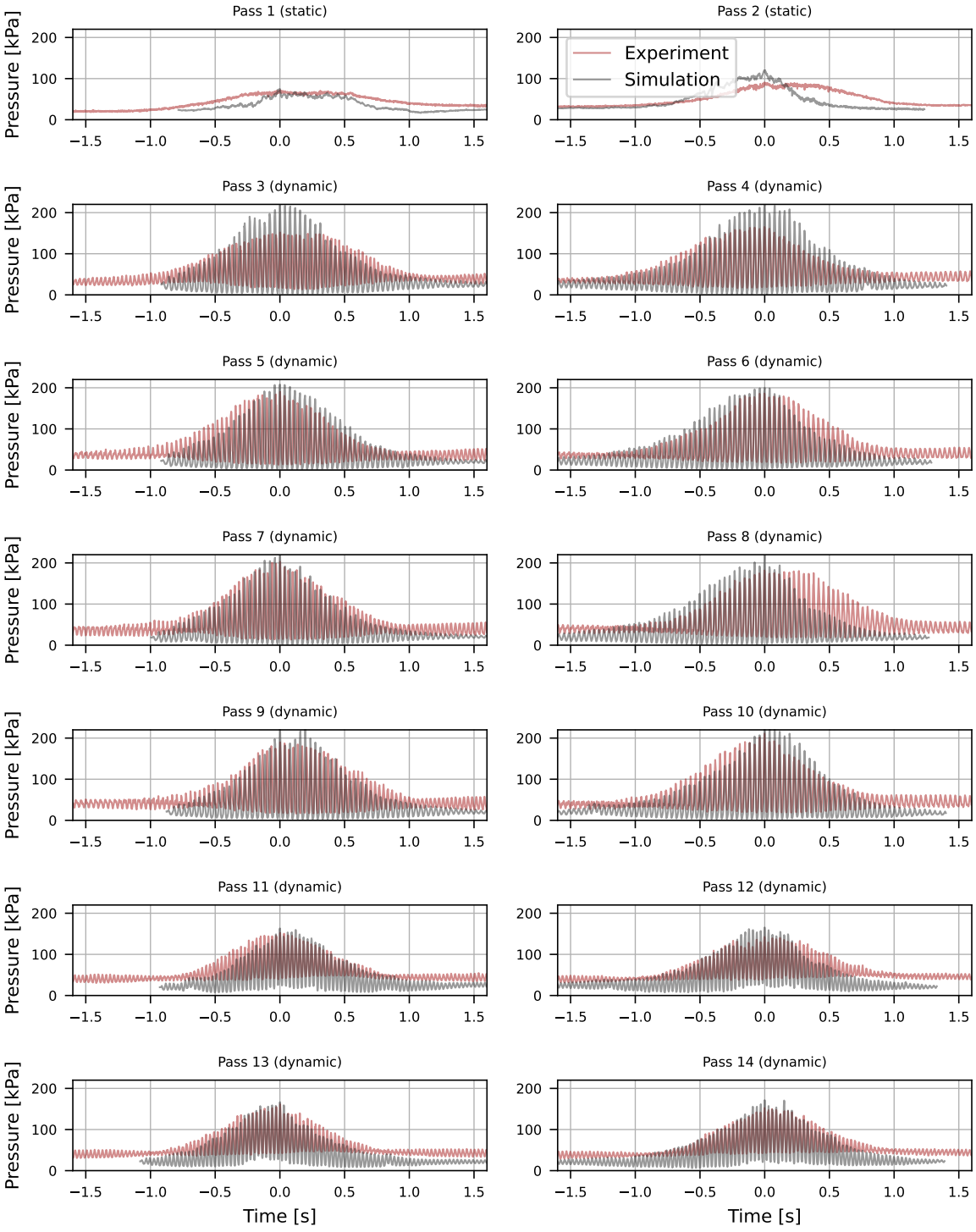


Figure 4.5. The ground pressure for each pass.

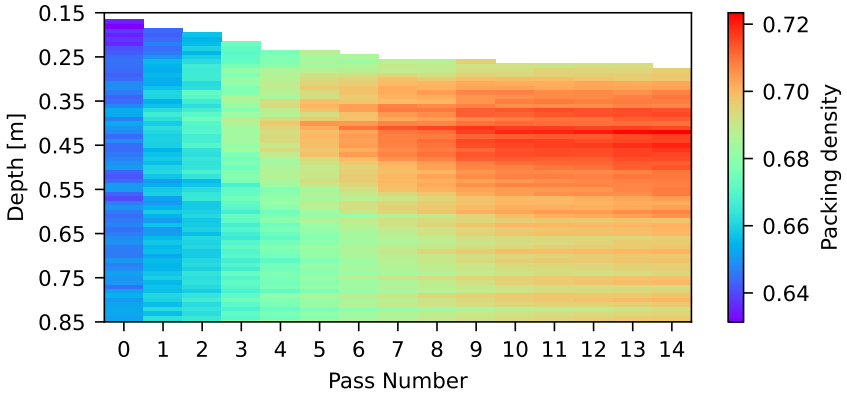


Figure 4.6. The packing density after each pass (in the simulation).

The results show that the packing density increases progressively with each roller pass, demonstrating the gradual densification of the material during compaction. However, the rate of increase decreases towards the final passes, indicating that the material is approaching a limiting packing state and that further densification becomes increasingly difficult to achieve. It can also be observed that the packing density is not uniformly distributed throughout the bed depth. Interestingly, the maximum packing density occurs at a depth of 0.4 m below the surface, rather than varying monotonically from the top to the bottom of the bed.

4.1.4. Discussion and future work

The validation demonstrated that coupled DEM–MBD simulations can realistically reproduce the dominant mechanisms governing vibratory roller compaction. The work also highlighted several modeling challenges. The results indicate that particle shape, particle interlocking and contact modeling have a significant influence on the predicted stiffness response. While the adopted particle representation successfully reproduced the overall compaction behavior, further improvements are likely possible through enhanced representations of particle interlocking and particle breakage.

An important advantage of the modeling framework is its ability to provide detailed information regarding the evolution of packing density, force transmission and force chain networks, and particle waves propagating through the medium. Such quantities are difficult to obtain experimentally but are highly valuable for understanding and optimizing compaction processes.

4.2. Validation of Coupled DEM–MBD Wheel Loader Simulations against Full-Scale Loading Experiments

4.2.1. Virtual product development

Virtual product development of heavy machinery is an important tool for manufacturers, where simulation models of the machines are used to give insights into their operation. These models may be used for design optimization and rapid evaluation of prototypes and new designs. One type of simulation that is commonly used in virtual development of heavy machinery is Multibody Dynamics (MBD), through which the dynamics of the machine in question may be modeled. For machines such as wheel loaders, excavators and articulated haulers, the interaction between the machine and some aggregate product is often of interest. The aggregate product may be modeled with high accuracy using the Discrete Element method (DEM). By running these two models as a two-way coupled co-simulation,

the interactions between the machine and the aggregate product can be studied.
In order to reliably employ such a coupled model in virtual product development, it is highly desirable to validate the model against experimental data, which gives insight into how well the model represents the real-world system. Such a validation is most often performed by comparing experimental data to equivalent data from the model.
A coupled DEM-MBD wheel loader model based on the Volvo CE L180 wheel loader has been developed, which is, for validation, compared to experimental data which were gathered at Volvo CE's test site in Eskilstuna.

4.2.2. Experiment setup

Physical experiments of the interaction between a wheel loader bucket and granular material have been performed at Volvo Construction Equipment's test site in Eskilstuna in order to obtain data which can be used for validation of a DEM-MBD model. A Volvo CE L180 wheel loader was employed for the experiments. 90 experiments in total were performed, with three replicates for each combination of bucket, size distribution and driving sequence. Table 4.1 presents all of these different parameters. For the *Normal* driving sequence the

Table 4.1. Wheel loader experiments parameters.

Size Distribution	Driving sequence	Bucket
M1 $(+0/-90)$	Normal	L150 $(4.0m^3)$
M2 $(+90/-150)$	Cheese slice	L180 $(4.6m^3)$
M3 $(+0/-150)$	In and up	-
M4 $(+4/-11)$	-	-
M5 $(+31.5/-63)$	-	-

operator filled the bucket in the manner that they would normally do it, for *Cheese slice* the operator followed the top edge of the pile with the bucket and for *In and up* the operator drove the bucket into the pile until stop and then lifted the bucket up.
A pocket which could be filled with granular material was constructed as seen in Figure 4.7. At the start of each experiment, the wheel loader was positioned like in the image, and then one of the driving sequences was initiated and the test stopped once the bucket had been loaded and the wheel loader had been stopped. For each of these 90 experiments, internal



Figure 4.7. Volvo CE test site pocket filled with granular material, along with wheel loader in starting position.

machine measurements were saved, along with a measure of the mass in the bucket after the driving sequence. A 3D scanning of the pile was done both before and after digging, which can provide information about the shape of the pile and how it changes during digging, along with a measure of total volume difference. An example of these scans are seen in Figure 4.8. Further, a 3D scan of the empty pocket was done before it was filled with material. A mesh was then created from this 3D scan, which, along with a photo of the pocket, is shown in Figure 4.9.

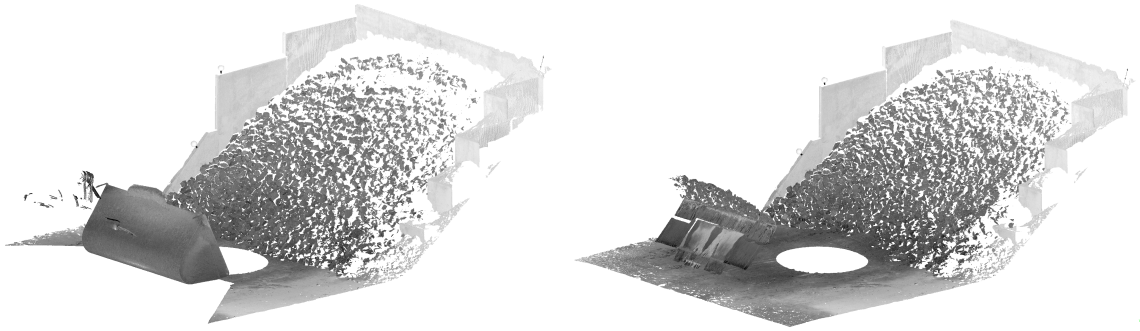


Figure 4.8. Example of 3D scans of pile before digging (right) and after digging (left).

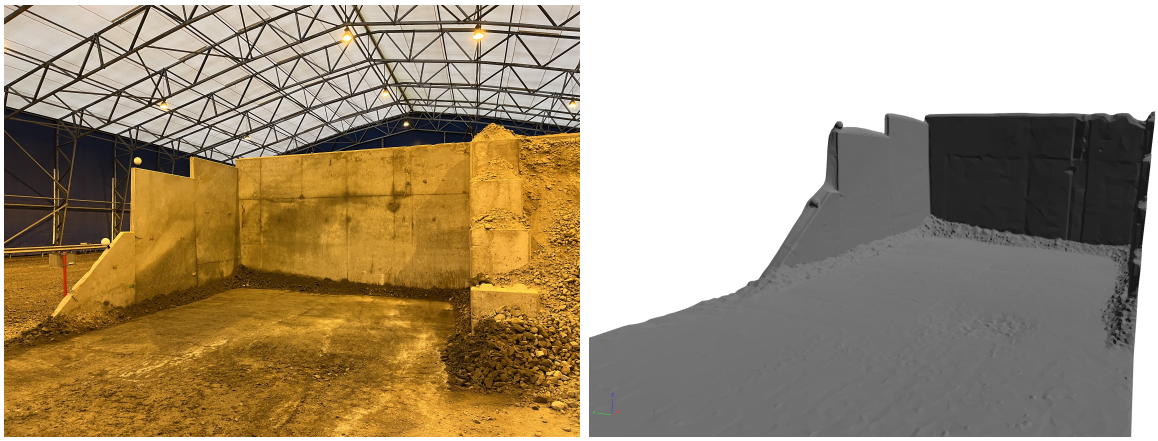


Figure 4.9. Empty test site pocket (left) and mesh representation of the pocket generated from 3D scans (right).

4.2.3. Simulation setup

A simplified Simulink Simscape MBD model of the wheel loader is employed, where the torque applied to each wheel is set through one scalar value per wheel, the full engine is thus not simulated. The hydraulics that are used for controlling the bucket are simulated in the MBD model, and are controlled through driver input signals of the tilt and lift of the bucket. These input variables for the wheel loader MBD model (bucket tilt and lift along with wheel torque) are retrieved from the experiments and imported into Simulink. This allows for a close comparison between the model and the experiments by ensuring that the same operator signals are used for both the experiments and simulations. A normalized example of these signals is seen in Figure 4.10.

This MBD model is coupled to a DEM model of the aggregate product of interest through a coupling scheme called Functional Mockup Interface (FMI). In this coupling the components of interest are coupled by the MBD model providing the motion of the part, which is applied to the corresponding component in DEM. The forces and torques acting on this DEM object are then calculated and communicated to the MBD model. Demify is used for the DEM model, in which the granular material is modeled and simulated. The particle geometries are given by 3D scanned rocks, from which the number of triangles are reduced and then

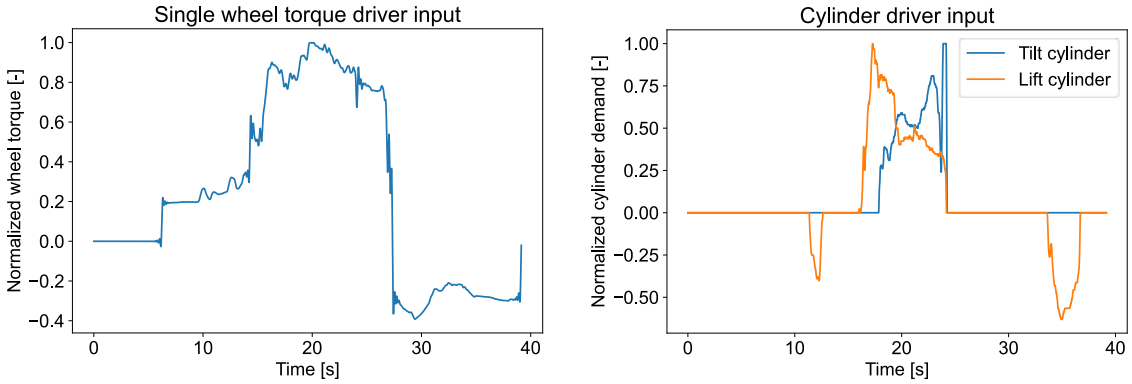


Figure 4.10. Normalized operator input signals.

the convex mesh of the particle is calculated. These three meshes are shown in Figure 4.11. A particle representation called dilated polyhedron is used for the particles, for which this convex mesh is used.

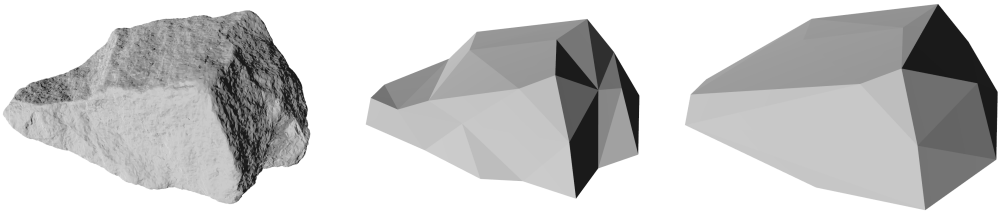


Figure 4.11. High resolution (left), low resolution (middle) and convex hull (right) meshes of a ballast particle.

A pile is created by generating particles above the mesh of the scanned pocket and letting the particles rain downwards until a pile has formed and settled. Two images of this pile along with all parts of the wheel loader that are coupled are shown in Figure 4.12.

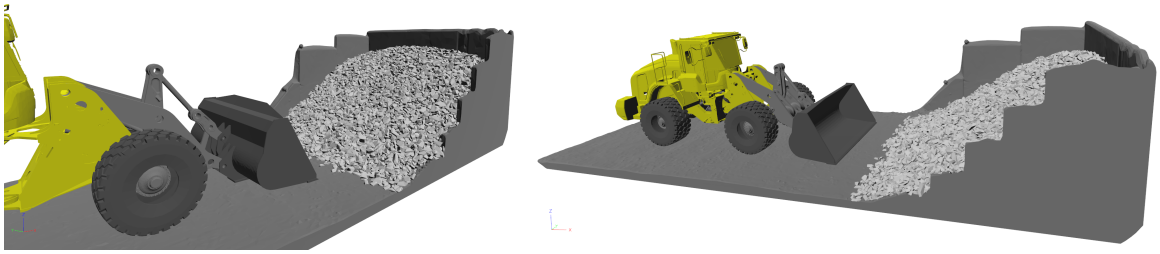


Figure 4.12. Full DEM model with pile and wheel loader. Wheel loader is at starting position.

4.2.4. Validation

For the validation of the coupled DEM-MBD wheel loader model, the simulations are limited to M2 (+90/-150) since the larger size distribution lends itself better to simulations because of the limited number of discrete particles. Further, only the largest bucket (L180) has been simulated, leading to 9 simulations in total, three replicates for each driving sequence.
In order to compare the experiments with the simulations, the same output measure from the experiments are retrieved from the simulations. The first of which is the total mass in the bucket at the end of the run. Figure 4.13 shows the mean mass in the bucket for each driving sequence along with the variance. For all three driving sequences the total mass in the bucket is higher for the simulation, along with a larger variance. This difference is very large for *In and up* and significantly smaller for *Normal* and *Cheese slice*.

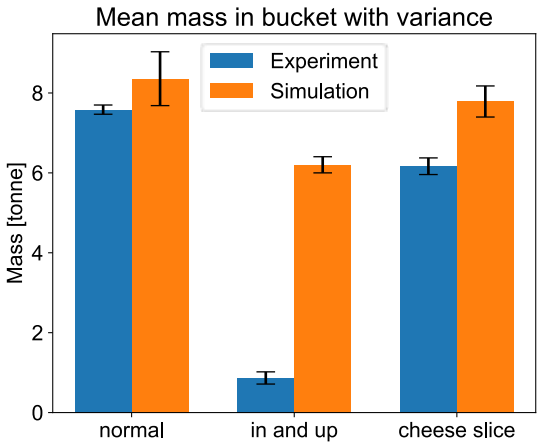


Figure 4.13. Comparison between experiments and simulations for the final mass in the bucket.

The 3D scans that were taken of the pile from before and after are post processed by discretizing the domain around the pocket in a grid in the x-y plane. The average height (along the z-axis) for each cell is calculated and then plotted where the height is given by the color. By performing this processing for the scans taken both before and after digging, a height-map of the change can be shown, where it can be seen how the pile has changed during digging. For the experiments, this is seen in Figure 4.14. The height-maps showing the difference between the pile before and after digging clearly shows where material has been taken from the pile. This difference looks quite similar for *Normal* and *Cheese slice* with some difference being seen in the size and depth of the affected area. Virtual 3D scans have been done for the simulations in order to obtain data which is comparable to the experimental data. Height-maps from these virtual 3D scans are shown in Figure 4.15. Both *Normal* and *Cheese slice* shows similar results as from the experiments, while there is a stark difference for *In and up*, where it looks very close to the other driving sequences for the simulation while there being very little discernible difference to be seen for the experiments. Figure 4.16 makes this comparison more clear by presenting the height-maps from both the experiments and the simulations side-by-side.

Analyzing the normalized pressures from the cylinders that control the bucket motion, the tilt and lift cylinder, shows that there are some differences between the experiments and the simulations, while some major features of the curves along with magnitude are captured for *Normal* and *Cheese slice*. *In and up* manages to capture some major features, however the magnitude is much higher in the simulations due to the increased amount of mass being loaded in the bucket. All of these plots are given in Figure 4.17.

4.2.5. Conclusions

The comparison between the experiments and simulations shows that for some driving sequences, the model is able to capture a lot of the behavior seen in a real-world experiment. Some parts of the model are not able to fully capture the real-world behaviors, mainly the simulations related to the *In and up* driving sequence. This difference between the experimental and simulated data seen for *In and up* could stem from the simplified MBD model. Since the model is simplified to only have a torque applied to each wheel, some parts of how the machine behaves may not be able to be accurate captured.

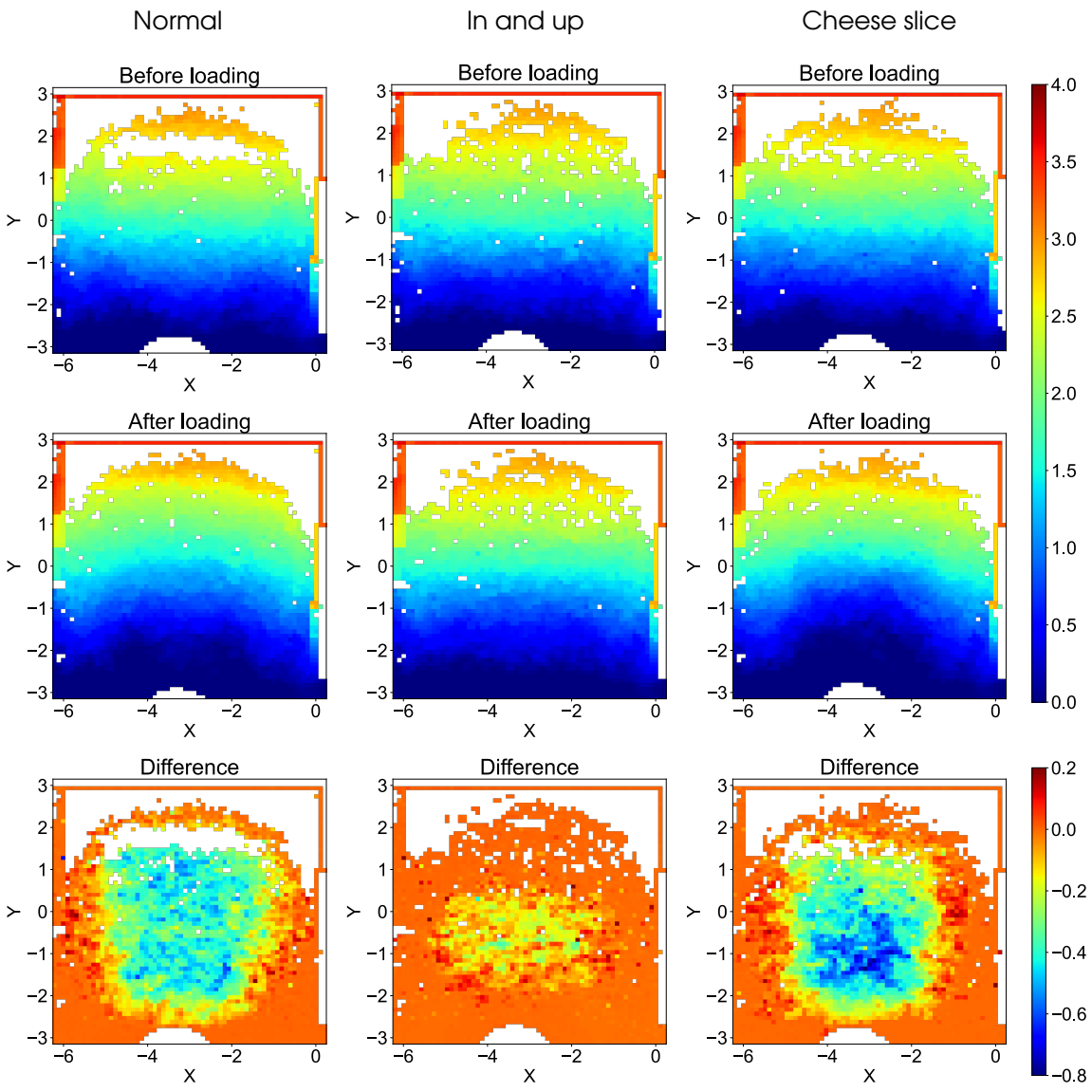


Figure 4.14. Experiment and simulation pile height-map for the three driving sequences.

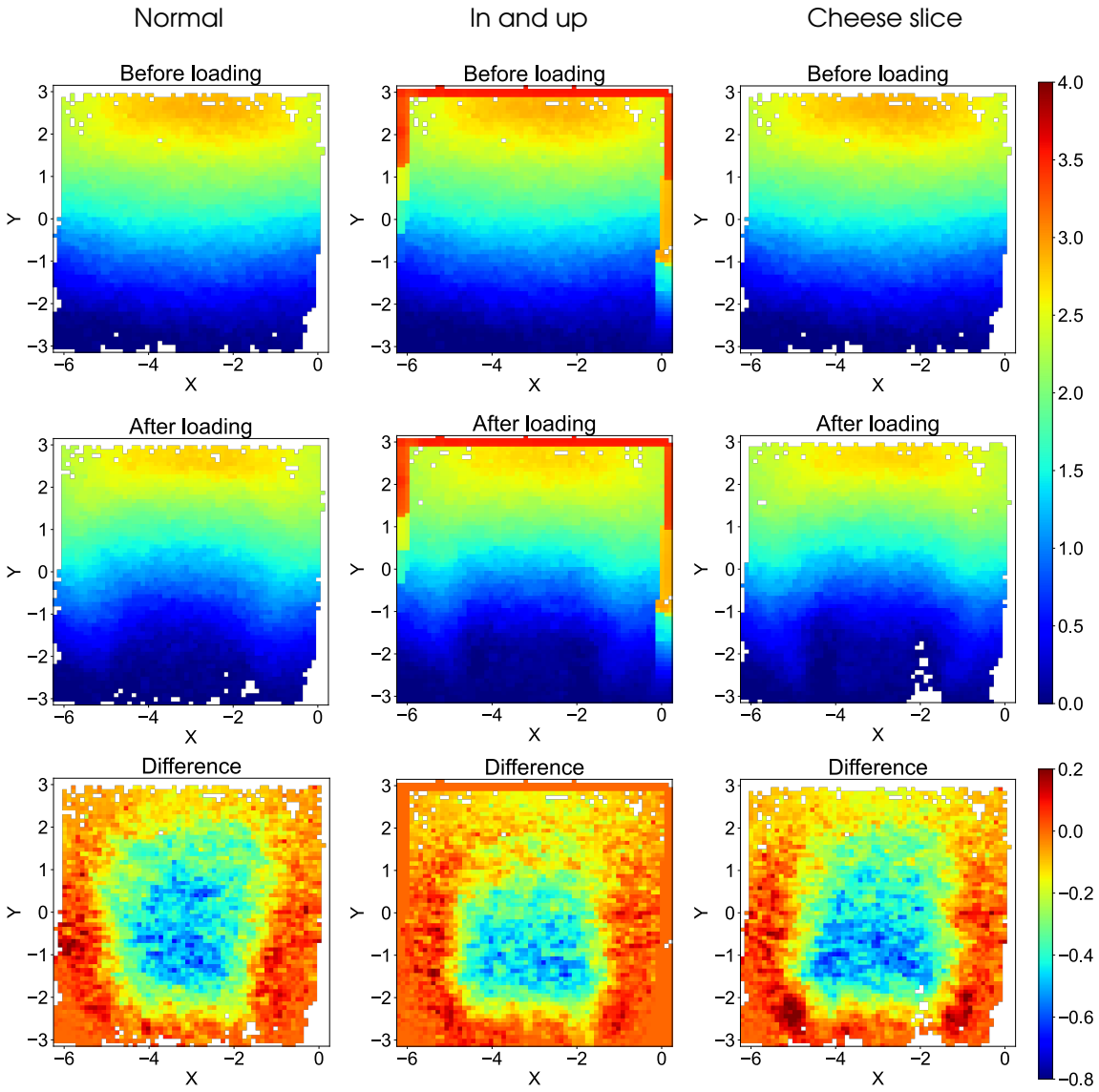


Figure 4.15. Simulation pile height-map for the three driving sequences.

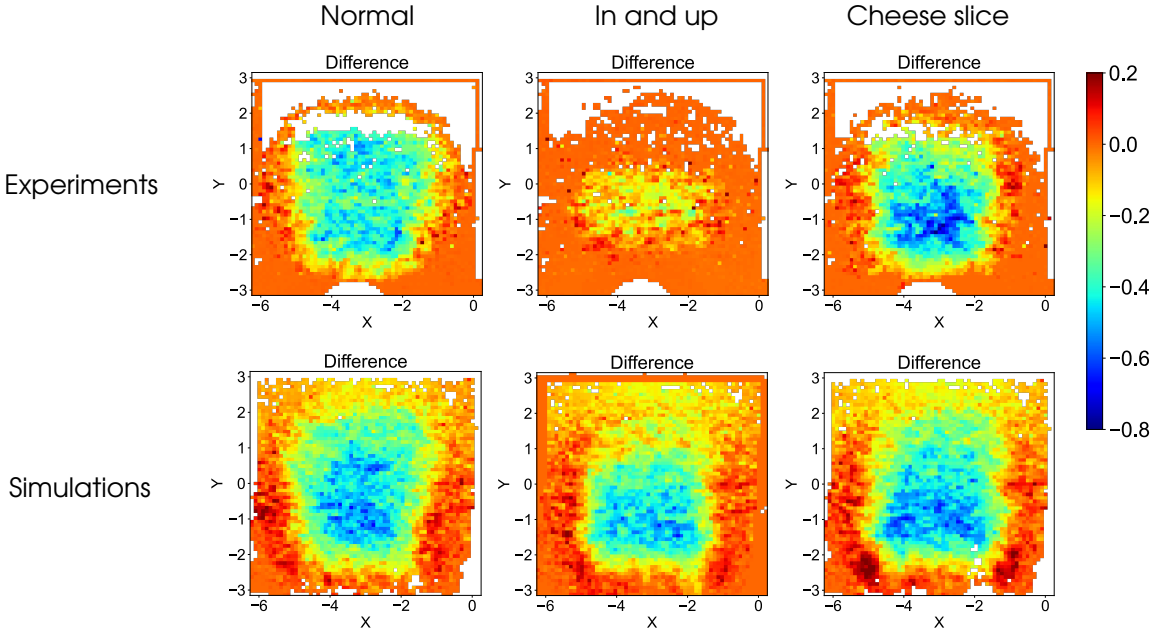


Figure 4.16. Experiment pile height-map for the three driving sequences.

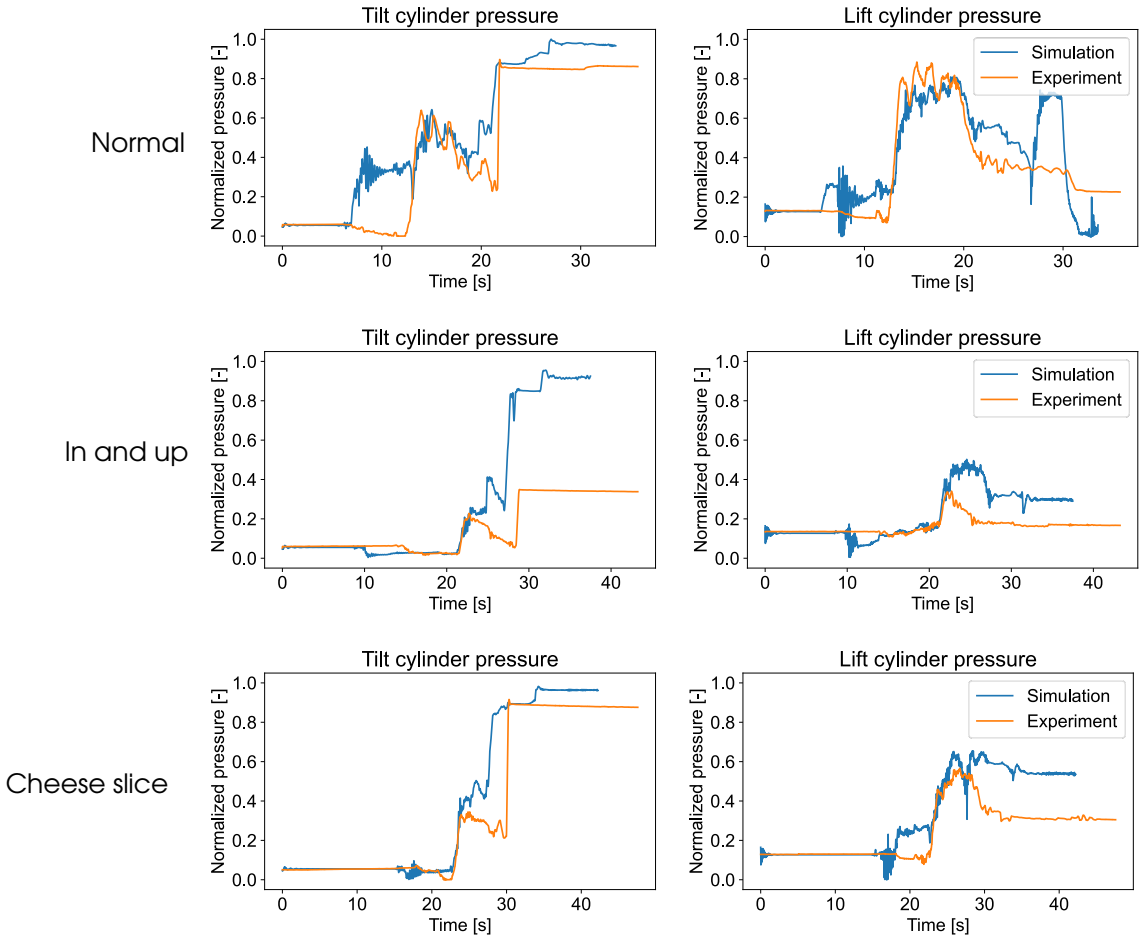


Figure 4.17. Tilt and lift cylinder pressure comparison between experiments and simulations.

5. Validation of Railway Structure Models under Operational Load Cases

An objective within DigiRail was to establish and validate experimental and numerical methods capable of investigating the mechanical behavior of railway ballast at both the component and the material scale. To support this objective, two test cases were considered in which simulations were performed and compared against measurements from experimental programs. First, the ballast behaviour was investigated in a sleeper push test and a cyclic oedometer. Thereafter, load transfer through the ballast bed was investigated in a trough bridge setup, all described in detail hereafter.

5.1. Experimental Validation of Ballast Behaviour and DEM Modelling

A complementary experimental and numerical programme was carried out focusing on the influence of ballast particle size distribution on stiffness, deformation, shear resistance and degradation behaviour. The work combined large-scale sleeper push tests, cyclic oedometer testing and corresponding DEM simulations. A more comprehensive description of the methodology, test programme and results is available in the SBUF project report 14488 [26].

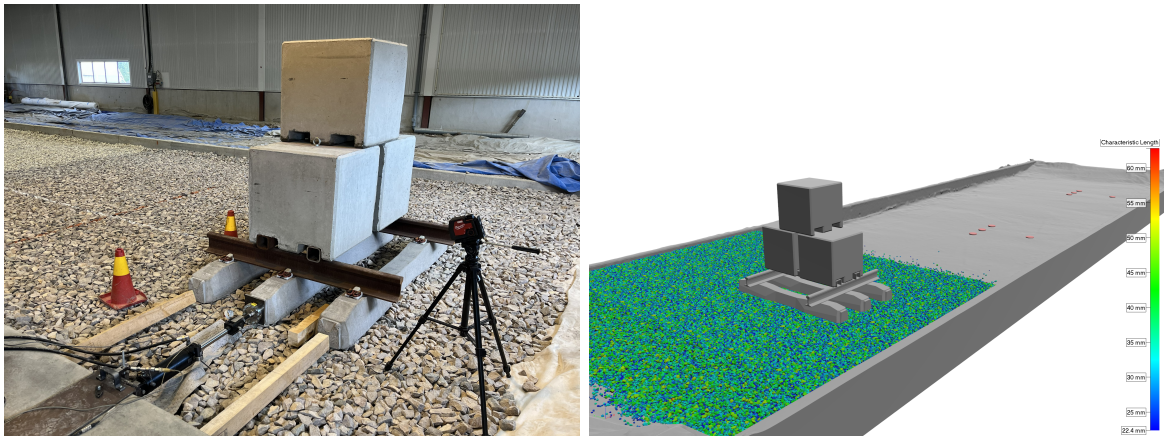
Three ballast materials with different particle size distributions were investigated. The reference material corresponded to a standard Class I railway ballast (M1), while two alternative gradings were selected to represent a broader grading (M2) and a bi-modal grading (M3/M3.2). The objective was not to identify an optimal grading, but rather to establish validated experimental and numerical methods and investigate how particle size distribution influences ballast behaviour.

5.1.1. Sleeper Push Tests and DEM Simulations

Figure 5.1a illustrates the experimental setup for the sleeper push test, while Figure 5.1b shows the corresponding DEM representation used for numerical simulations. The sleeper push test was developed as a large-scale experimental method for studying ballast shear behaviour and lateral track resistance under controlled loading conditions. The test configuration consisted of three concrete sleepers placed in a ballast bed, where the centre sleeper was subjected to horizontal displacement using a hydraulic loading system while the outer sleepers provided a representative support condition.

The test programme included several combinations of vertical loading and confinement conditions. Vertical loading was applied through the self-weight of the sleeper system together with additional concrete blocks placed above the rails. Two different confinement conditions were investigated, providing insight into the influence of ballast shoulder support and lateral restraint. The developed test method enabled repeatable measurements of force-displacement behaviour up to sleeper displacements of approximately 50 mm.

The measured responses exhibited a characteristic behaviour consisting of an initial rapid force increase followed by a gradual transition towards a stable resistance level. Across all



(a) (b)

Figure 5.1. Sleeper push tests. (a) Test setup with three concrete blocks and (b) illustration of the DEM model for the sleeper push test.

materials, the dominant factors controlling the response were the applied vertical load and the degree of confinement. Increasing confinement and vertical loading resulted in higher lateral resistance and increased apparent shear strength. Differences between particle size distributions were observable but generally smaller than the influence of the boundary conditions.

A Mohr-Coulomb interpretation of the experimental data showed relatively small variations in friction angle between the investigated gradings. In contrast, confinement had a significant influence on the apparent cohesion. The results indicate that ballast confinement and packing state are more important for the mobilized shear resistance than moderate variations in particle size distribution.

To complement the experiments, DEM models of the sleeper push test were developed using the Demify framework. The simulations explicitly represent ballast particles using dilated polyhedral particle shapes and include detailed geometric representations of the sleeper system and loading arrangement, as shown in Figure 5.1b. A calibration study was first performed to identify suitable contact parameters governing particle-particle and particle-sleeper interactions. Following calibration, simulations were conducted for the investigated ballast materials and compared with experimental measurements.

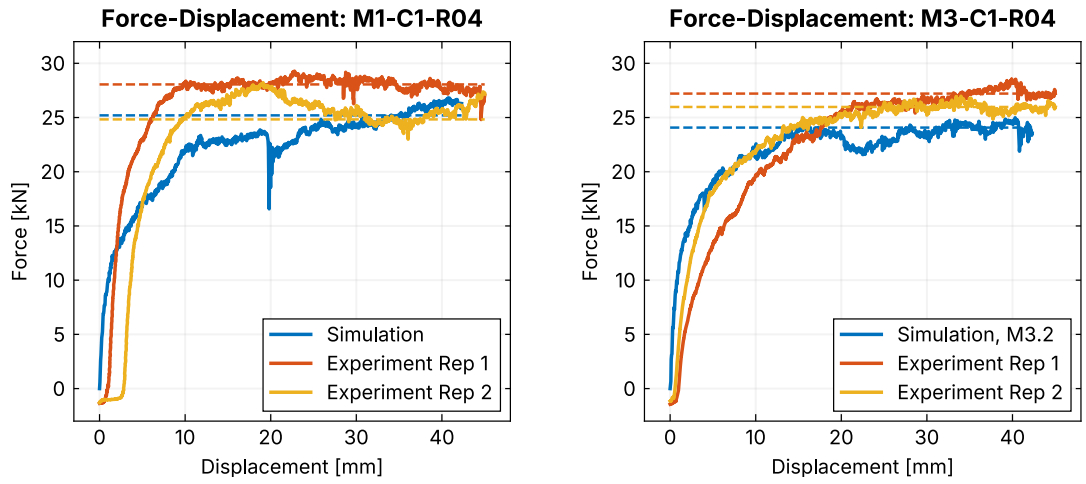
Figure 5.2 compares measured and simulated force-displacement responses for two representative ballast gradings. The DEM simulations reproduced the principal characteristics of the response and captured the relative differences between the investigated materials. In particular, the agreement is good for the asymptotic resistance levels, providing confidence that the numerical model realistically represents the dominant mechanisms governing ballast shear behaviour.

The simulations also provide access to information that is difficult to measure experimentally, including particle rearrangement and force transmission within the ballast bed. These analyses showed how variations in grading influence load transfer pathways and the development of force chains during loading.

5.1.2. Cyclic Oedometer Tests and DEM Simulations

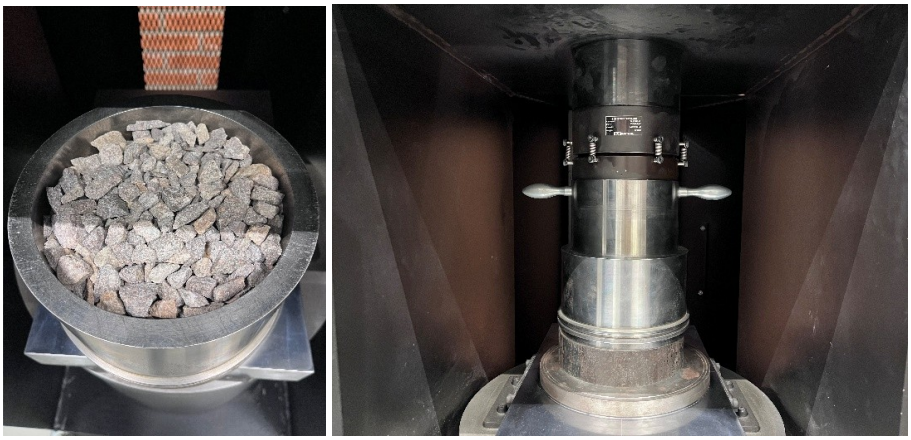
In addition to the sleeper push tests, cyclic oedometer experiments were carried out to investigate ballast deformation, stiffness development and material degradation under repeated loading. The tests were performed in a rigid cylindrical container shown in Figure 5.3 where ballast specimens were subjected to cyclic vertical compression while lateral expansion was restrained.

Due to the dimensions of the laboratory apparatus, the ballast gradings were geometrically



(a) (b)

Figure 5.2. Force-displacement comparison of simulation and experiments for (a) M1, and (b) M3.2.



(a) (b)

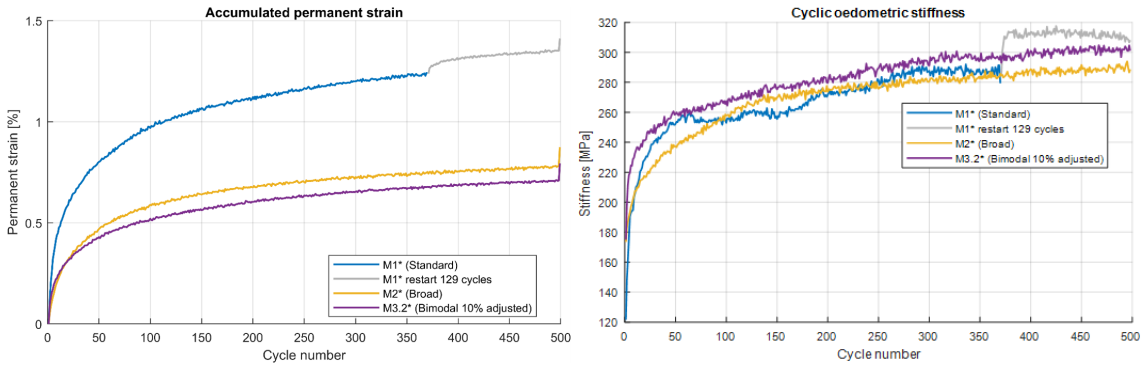
Figure 5.3. (a) Picture of the cylinder for the oedometer test setup with the prepared sample, and (b) loading arrangement in the Instron test rig.

scaled while preserving the overall shape of the particle size distributions. The tests included repeated loading cycles up to stress levels representative of railway loading conditions. Throughout the experiments, vertical stress and deformation were continuously monitored, allowing the evolution of permanent strain and stiffness to be evaluated.

All materials exhibited the expected behaviour of granular railway ballast: rapid deformation during the initial loading cycles followed by progressive densification and increasing stiffness. Figure 5.4 summarizes the evolution of permanent strain and oedometric stiffness during cyclic loading. The standard ballast grading (M1) exhibited the largest permanent deformation and showed the most pronounced particle size redistribution after testing. In contrast, both the broad grading (M2) and the bi-modal grading (M3.2) exhibited lower permanent deformation and reduced overall degradation.

Analysis of the post-test particle size distributions revealed that the initial grading strongly influences ballast fragmentation behaviour. M1 produced the highest overall level of degradation, whereas M2 and M3.2 showed lower breakage indices. At the same time, the bi-modal grading generated relatively high amounts of fine material despite a lower overall breakage level, indicating a different fragmentation mechanism compared with the other materials.

A corresponding DEM representation of the oedometer test was developed to investigate the observed behaviour at particle scale and is shown in Figure 5.5. The simulations reproduced



(a) (b)

Figure 5.4. Results from cyclic oedometric loading tests for materials M1, M2, and M3.2: (a) accumulated permanent strain as a function of cycle number and (b) cyclic oedometric stiffness as a function of cycle number. Illustrating progressive stiffening and convergence toward a stabilized response with increasing loading cycles.

the geometry and loading conditions of the laboratory experiments and utilized the same particle representation and contact formulations as the sleeper push studies.

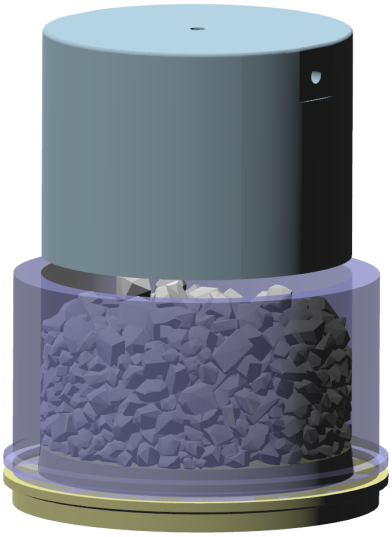


Figure 5.5. Illustration of the oedometer rig in the DEM model.

Although the simulations did not explicitly include particle breakage, they successfully reproduced the relative trends observed experimentally. In particular, the simulations predicted larger deformation for M1 and higher stiffness for M2, consistent with the laboratory measurements. Figure 5.6 illustrates the evolution of simulated bed stiffness, showing the same material ranking as observed experimentally.

The DEM results also provided a mechanistic explanation for these differences. The broader grading distributed the applied load across a larger number of particles and contacts, resulting in lower peak contact forces. In contrast, the standard grading generated a larger proportion of highly loaded contacts, leading to more localized force transmission and a greater propensity for deformation and degradation.

5.1.3. Conclusions and Future Work

The combined experiments and DEM simulations showed that ballast particle size distribution influences deformation, stiffness and degradation behaviour. The numerical models

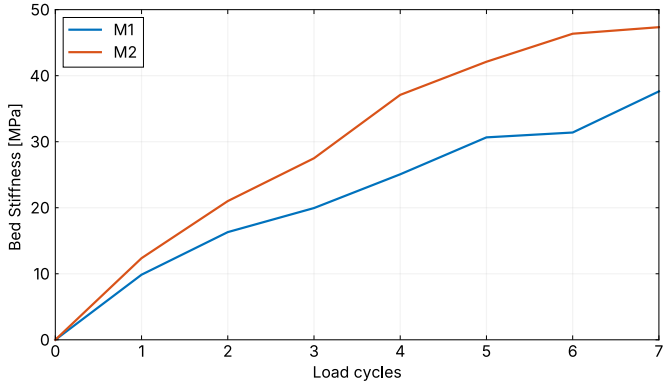


Figure 5.6. Bed stiffness for two of the materials M1 and M2 with a scaled particle size distribution.

successfully reproduced the main trends observed in the laboratory tests and provided insight into the underlying particle-scale mechanisms.

Future work should focus on incorporating particle breakage into the DEM framework and applying the validated methodologies to larger railway-system simulations within the DigiRail modelling framework. The established experimental and numerical platform also enables more systematic investigation of alternative ballast particle size distributions and particle characteristics, supporting future studies aimed at improving ballast performance and long-term track behaviour.

5.2. DEM-FEM Simulations of a Trough Bridge

Following the investigation of ballast behaviour and its representation in the Discrete Element Method (DEM), the next step was to evaluate the DEM-FEM modelling approach against experimental data from a real-world application. The trough bridge experimental campaign was conducted at Luleå University of Technology as part of the Trafikverket funded project *Full scale laboratory test of trough bridges*. Measurements obtained during this campaign were compared with DEM-FEM simulations replicating the same trough bridge configuration. The primary objective of this study was to assess the influence of the ballast particle bed on the pressure distribution acting on the trough bridge structure.

A detailed description and analysis of the experimental setup and results are given by Sarmiento et al. [20] and Sarmiento [27]. The trough bridge was cast based on the geometry and reinforcements typical for bridges along the Iron Ore Line. After installment of the bridge in the laboratory, the bridge was instrumented with various sensors, among other 24 load plates. The bridge was subjected to 20 million load cycles during 24 load stages, each stage entails four load cases. The first three load cases induced a static load with three different configurations of the axle positioning. The last load case then consists of cyclic loading with 1 million cycles. 14 stages has been performed before the ballast was exchanged. The comparison between the experiments and simulations presented hereafter focuses on the first load case of stage 15, where a single axis, positioned close to the center of the bridge, is subjected to a static load. A photograph of the bridge is shown in Figure 5.7, where the axle positioning corresponds to the first load case.

5.2.1. Method

To model the entire trough bridge with all the structural objects as shown in Figure 5.8 and resolving the single particles in the particle bed, the DEM-FEM coupling, previously applied for simulations of a trough bridge segment in Eriksson et al. [28], has been used.

The ballast bodies have been created as an assembly of convex dilated polyhedra, while the sleepers, rails, trough, supports, and metal plates are defined as FE objects in the coupled



Figure 5.7. Photograph of the experimental rig of the trough bridge at Luleå University of Technology.

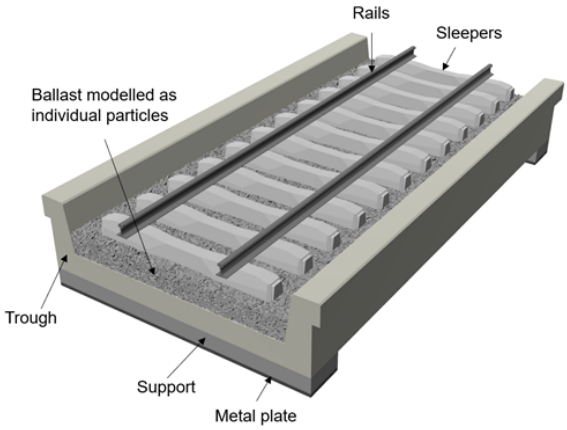


Figure 5.8. Illustration of the trough bridge model with all structural objects included in the simulation.

model. These objects were created according to the experimental specifications, yet the trough bridge was modelled without reinforcement.

At the supports of the trough bridge, clamp boundary conditions were applied restricting displacement and rotation entirely at one side and restricting movement in vertical direction on the other side. For the rails a symmetry boundary condition was applied in longitudinal direction. The ballast is restricted in the longitudinal direction by walls. The load is applied as pressure on the rails at the position corresponding to the experiment. A value of 250 kN corresponding to the static load case is divided by the rail seating area on both sides to obtain pressure.

5.2.2. Results

For the comparison of the surface pressure distribution on the trough bridge, stage 15 was chosen as this represents the fresh ballast case. The comparison of case I with static loading is shown in Figure 5.9. From this comparison, it can be seen that the pressure in both simulation

and experiment is in the same order of magnitude, yet the pressure on the trough bridge calculated in DEM-FEM is more evenly distributed over the area below the sleeper above which the load was applied and its direct neighbours.

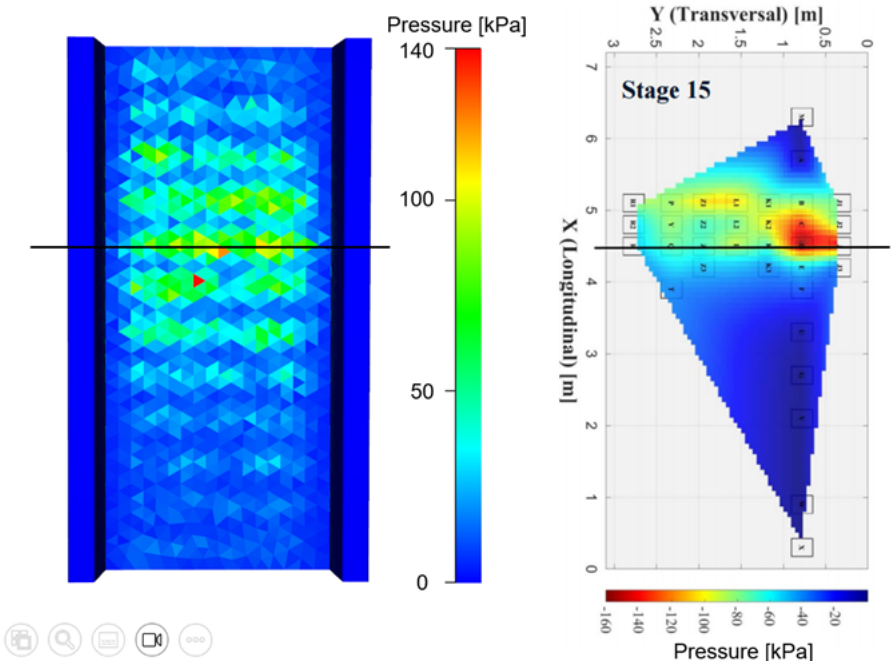


Figure 5.9. Side-by-side view of the simulation results (left) and the measurements (right) from the static load case I at stage 15. Note that the color bars are not identical due to software restrictions.

One great advantage of DEM-FEM simulations is the possibility to easily modify the particle bed and test different bed characteristics but also different instantiations of the same bed characteristics to obtain statistical information. For further comparison, several instantiations of the particle bed were generated and tested under cyclic loading. Three representative simulations are shown in Figure 5.10. It is visible that although the modelling setup is identical, statistical random filling of the particles leads to varying pressure distributions on the trough bridge surface, where also asymmetric pressure distributions occur.

5.2.3. Discussion and Conclusion

The particle bed and its packing show a strong influence on the surface pressure distribution on the trough bridge. This is evident as different realizations of the particle bed produce slightly different surface pressure distributions. Although the differences are not very pronounced, a clear asymmetry sometimes occurs in the simulations, which is also visible in the experimental measurements.

This observation is noteworthy since structural design of trough bridges commonly assumes that loads from sleepers are transferred to the supporting structure in a largely symmetric manner. The present results indicate that the discrete nature of the ballast bed may lead to stochastic load paths and the formation of force chains, resulting in asymmetric pressure distributions on the bridge surface even under symmetric loading conditions. In practice, this suggests that local peak loads on the trough structure may deviate from those predicted by simplified symmetric load assumptions. Further systematic studies are therefore required to quantify the statistical variability of these pressure patterns and evaluate their implications for structural dimensioning.

Characterising the particle bed under pre-compacted and loaded conditions is challenging, yet the influence of packing density is significant. A continuation of the collaboration is anticipated in which the 3D scanned particle bed serves to characterize the particle bed, which can be reproduced in the simulations. Additional static and cyclic load experiments

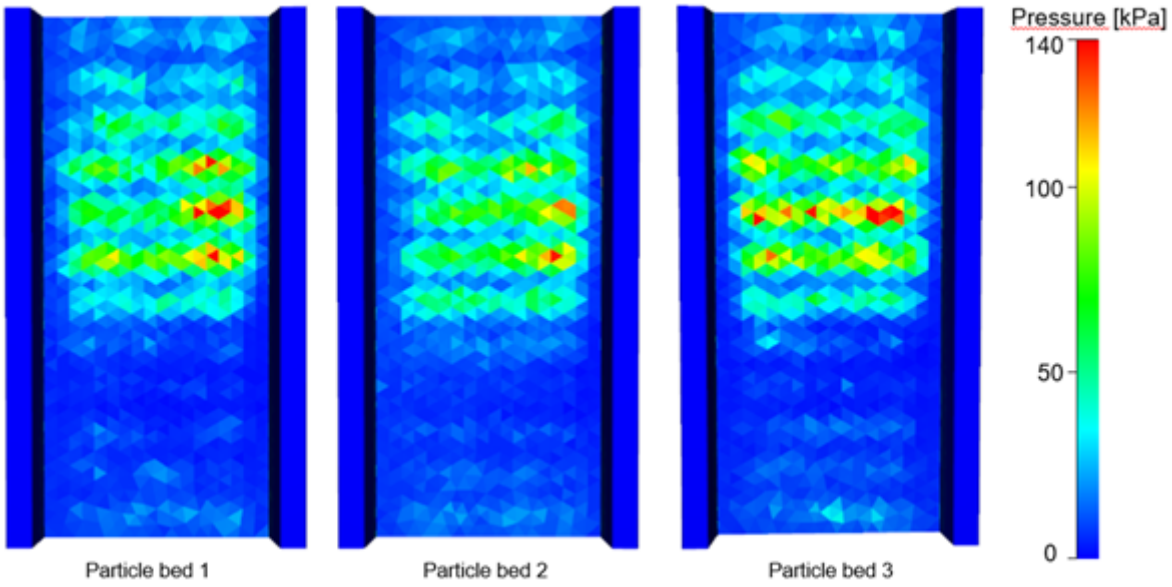


Figure 5.10. Surface pressure distribution on the trough bridge for three different particle bed instantiations with identical bed characteristics from case I under cyclic load at stage 15.

that meet the performance capability of the simulations allow a best-possible one-to-one comparison between simulation and experiment, thereby increasing confidence in the modeling setup.

6. Validation and Investigation of Critical Maintenance Operations

6.1. Background

Maintaining railway track geometry is essential for ensuring safe, reliable, and cost-effective railway operations. Under repeated traffic loading, the ballast bed gradually degrades and settlements occur, leading to geometric irregularities in the track. These defects increase dynamic wheel-rail forces, accelerate infrastructure degradation, and eventually require corrective maintenance. Tamping remains the most common maintenance operation for restoring track geometry by lifting the sleepers and compacting ballast beneath them using what is called tamping tines. In order to decrease the forces needed to insert the tamping tines into the ballast bed, vibrations are induced in the tines. However, tamping itself contributes to ballast degradation through particle breakage and abrasion, creating a trade-off between restoring track geometry and preserving ballast quality. An example of a tamping machine is seen in Figure 6.1.

Conventional tamping machines generate tine vibrations using an eccentric shaft, a concept that has remained largely unchanged for decades. More recently, fully hydraulic tamping systems have been introduced, such as the fully hydraulic tamping bank developed by System7. By generating vibrations directly through hydraulic actuation, these systems enable independent control over the vibrations and the tamping sequence. Further, by measuring the pressure and travel distance in the cylinders, more sophisticated tamping criteria can be used. Conventional tamping machines typically perform the tamping operation for a set period of time, usually around one second, while for one of the aforementioned hydraulic tamping machines the time may vary based on the state of the ballast bed.

The objective of this work was to develop a coupled numerical framework capable of simulating both the ballast bed and the dynamic behavior of a tamping machine. The framework was then used to compare conventional and fully hydraulic tamping concepts.

6.2. Development of the Co-Simulation Framework

To capture both ballast behavior and machine dynamics along with their interactions, a two-way coupled DEM-MBD co-simulation framework was developed. The ballast bed was represented using DEM in Demify, while the tamping machine was modeled using Multibody Dynamics in Simscape Multibody. The simulations were coupled through the Functional Mockup Interface (FMI), allowing force and motion data to be exchanged during runtime.

The overall simulation setup is illustrated in Figure 6.2, which shows the tamping machine together with the ballast bed and sleepers. The model represents the key physical interactions occurring during tamping: vibrating tines penetrate the ballast bed, move toward each other, and compact the ballast beneath the sleeper while interacting with individual ballast particles.

The ballast particles were represented by simplified polyhedral shapes derived from scanned ballast stones, as seen in Figure 4.11. The particle size distribution follows the Swedish ballast

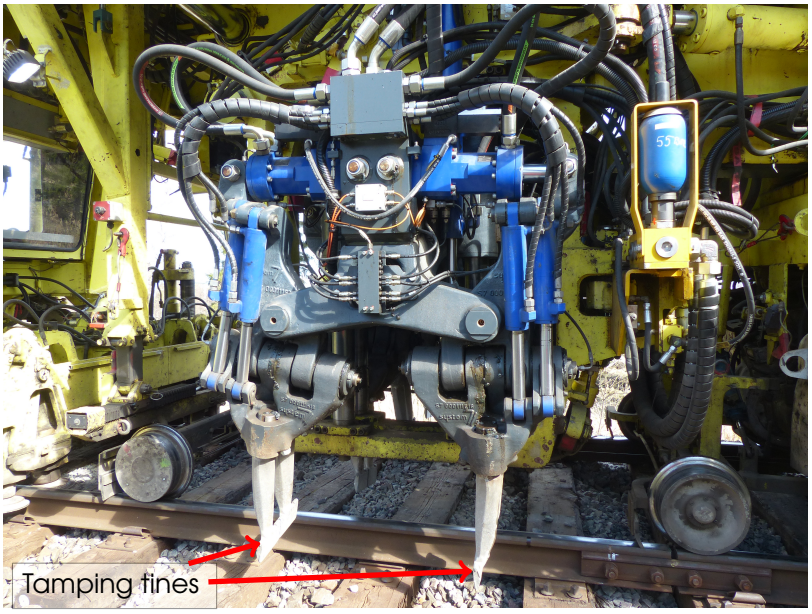
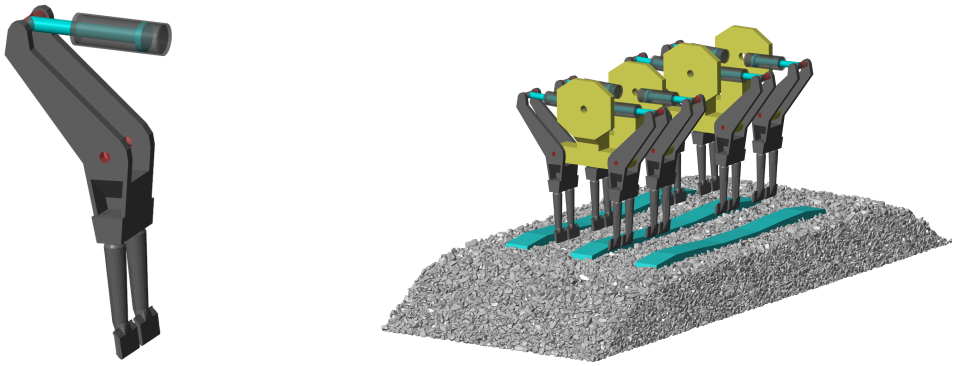


Figure 6.1. Fully hydraulic tamping machine.



(a) Tamping arm with hydraulic cylinder.

(b) Tamping bank and ballast bed models.

Figure 6.2. MBD and DEM model of tamping machine and ballast bed.

grading requirements and material properties such as, stiffness, friction, and restitution were used from the previously described direct shear calibration. The ballast section consisted of three sleepers and the surrounding ballast bed, providing sufficient space to study local compaction effects while maintaining manageable computational cost.

Two separate tamping models were developed, one for the fully hydraulic machine and one for the conventional machine. These models differ in that the vibrations in the hydraulic model are generated by the hydraulic cylinders while the full eccentric mechanism is modeled for the conventional machine. The tamping criteria is also different for the two models, the conventional machine performs the tamping operation for one second, while the fully hydraulic model tamps until a certain packing density criteria is met. This criteria was chosen to be 0.68 in this project.

6.3. Model Calibration

Before comparing tamping concepts, the hydraulic model was calibrated against real-world data from System7's online tool Inframe, where data from a fully hydraulic tamping machine is logged during the tamping operation. This data was provided to this project through Infranord. Calibration focused on compaction force and squeeze path, two quantities that describe both machine performance and ballast response. These two variables are

measured in the tamping cylinders, where the compaction force is the average value of maximum forces measured in each individual cylinder. Similarly, the squeeze path is the average value of the maximum travel distance measured in each individual cylinder. The calibration study was performed to identify an appropriate damping coefficient representing resistance in the hydraulic system.

Simulation results were compared against a data of recorded tamping operations. Rather than reproducing a single measurement, the aim was to ensure that the numerical model produced responses within the distribution observed in practice. Figure 6.3 shows the distribution of both compaction force and squeeze path from the real-world data along with the mean of this data and the values from the calibrated model. The calibrated model successfully reproduced squeeze paths and compaction forces close to the mean of the real-world data and therefore provided confidence in the predictive capabilities of the proposed co-simulation framework.

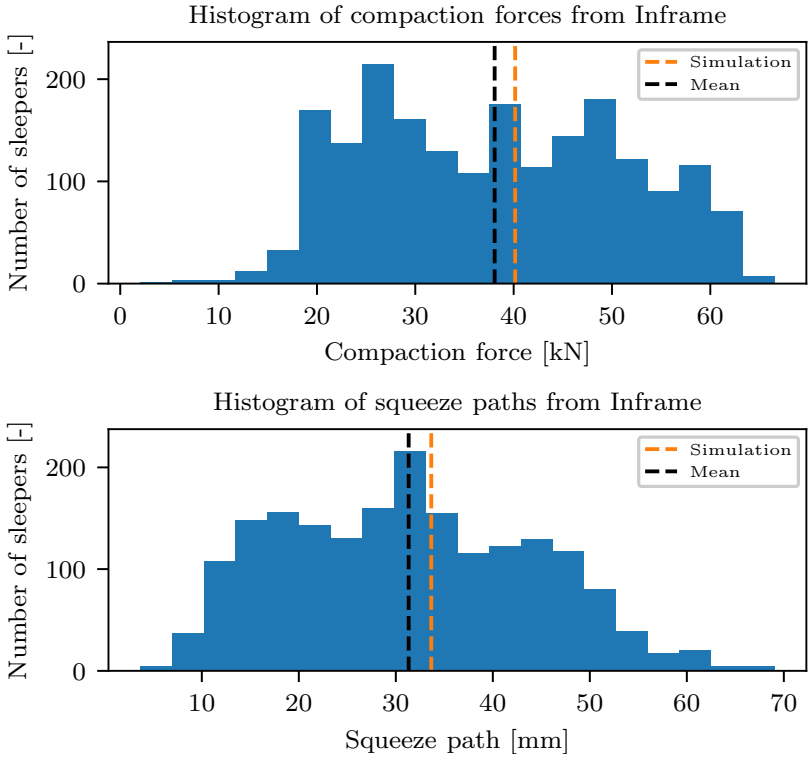


Figure 6.3. Distribution of compaction force and squeeze path along with calibrated simulation results and mean of experimental data.

6.4. Results

The primary comparison examined conventional and fully hydraulic tamping systems under identical nominal operating conditions. Performance was assessed using packing density beneath the sleeper, packing density beside the sleeper, and force exposure of ballast particles.

The evolution of packing density is shown in Figure 6.4. This figure is one of the most important results of the study because it directly quantifies ballast compaction effectiveness.

Both tamping concepts increased the packing density beneath the sleeper. However, the hydraulic system maintained more effective compaction throughout the squeezing phase and achieved a higher final packing density. The fully hydraulic model achieved a final density of approximately 0.684 compared with approximately 0.679 for the conventional case. Similar trends were observed beside the sleeper.

Although the numerical differences appear small, they are significant because packing

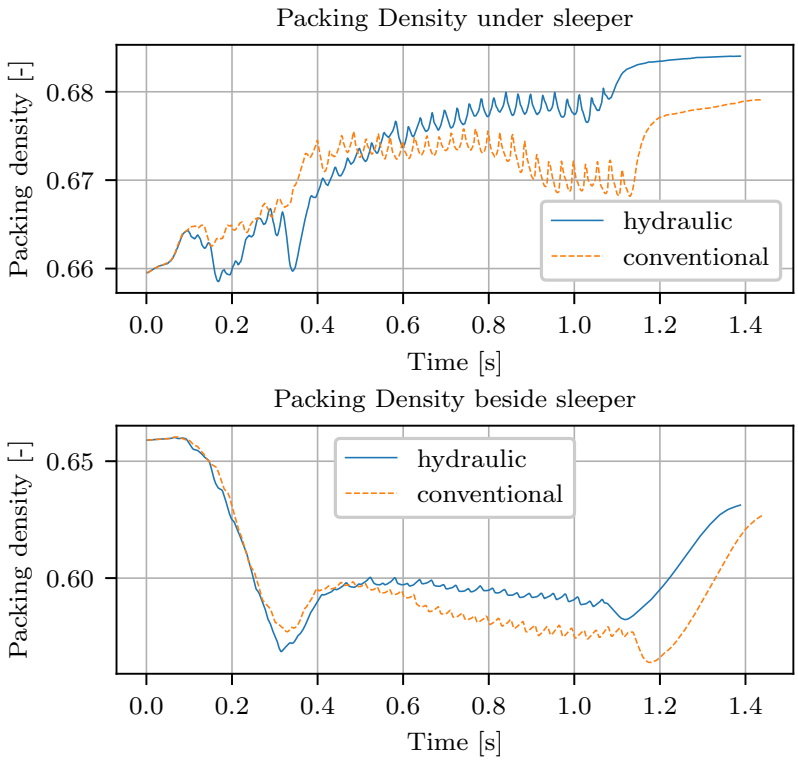


Figure 6.4. Packing density beneath the middle sleeper (top) and beside the sleeper (bottom) for both tamping models.

density is directly related to load transfer capability and ballast stability. A higher packing density indicates improved interlocking between ballast particles and a stronger support structure beneath the sleeper.

Compaction quality must be considered together with ballast degradation. Excessive particle loading can increase breakage and wear, reducing long-term track quality.

The distribution of maximum particle forces experienced during tamping is presented in Figure 6.5.

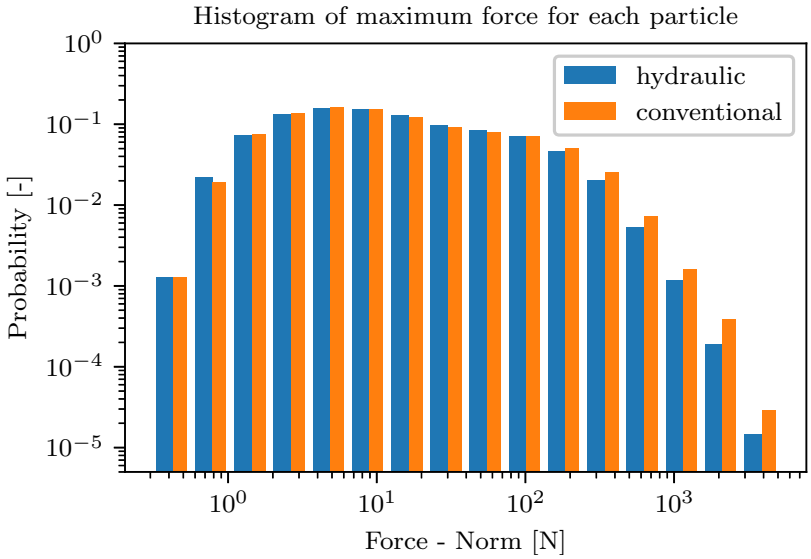


Figure 6.5. Distribution of maximum force acting upon each particle for both tamping models.

The hydraulic tamping concept resulted in a larger proportion of particles experiencing relatively low forces and a smaller proportion experiencing high forces. In contrast, the conventional tamping model produced a larger number of particles subjected to loads

above 100 N. These results indicate a higher risk of particle breakage and abrasion in the conventional case.

6.5. Conclusions

The most important outcome of this study is the demonstration that a fully coupled DEM-MBD framework can capture the interaction between tamping machine dynamics and ballast behavior with some degree of realism.

The comparison between tamping concepts indicates that fully hydraulic tamping provides advantages over conventional eccentric-driven systems. The hydraulic approach achieved higher packing densities beneath and beside the sleeper while simultaneously exposing ballast particles to lower contact forces. This combination is particularly valuable because it addresses both short-term maintenance effectiveness and long-term ballast preservation.

Ultimately, this work demonstrates that tamping optimization should not focus solely on restoring track geometry. Equally important is the reduction of ballast degradation, as this directly influences maintenance intervals and lifecycle costs. The developed simulation framework provides a powerful tool for evaluating future machine concepts and operating strategies before field implementation.

7. Investigation of Transition Zones and Verification against Analytical Calculation Methods

7.1. Application of the Transition Zone Model to Högsjö Västra

The developed transition zone simulation framework was applied to an existing railway infrastructure project at Högsjö in Sweden. The Högsjö Västra project concerns the construction of two passing tracks along the Västra stambanan, approximately 3.5 km north of Högsjö. The Västra stambanan between Gnesta and Hallsberg is a double-track railway line with significant capacity constraints, which have limited the ability to accommodate both passenger and freight traffic and resulted in delays associated with train crossings and overtaking. The planned intervention comprises approximately 2.3 km of new track infrastructure, together with service roads required for construction and maintenance.

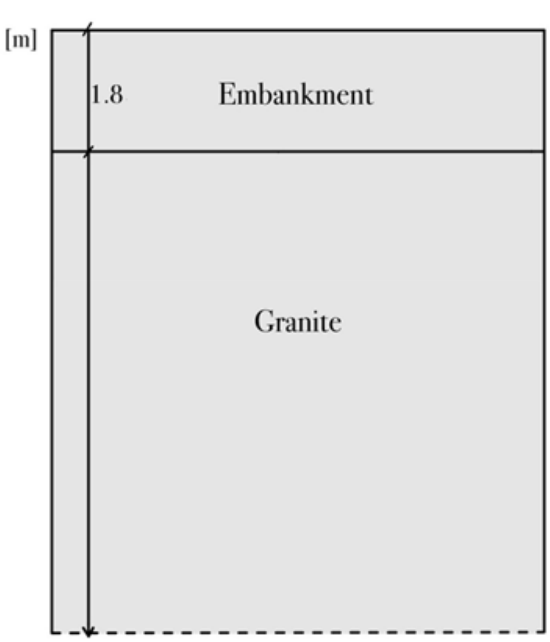
The Högsjö project provides a representative case for applying the developed DEM-FEM framework to an actual railway infrastructure project. The available project documentation and site-specific information provide a basis for modelling realistic track configurations and transition zones. The case study therefore provides an opportunity to assess the applicability of the developed framework to infrastructure planning and its potential use as part of an engineering workflow for evaluating railway transition zones. The objective was to assess whether the framework can be used to evaluate different transition-zone designs and their influence on the dynamic loads transferred to the track structure.

7.1.1. Simulation Model

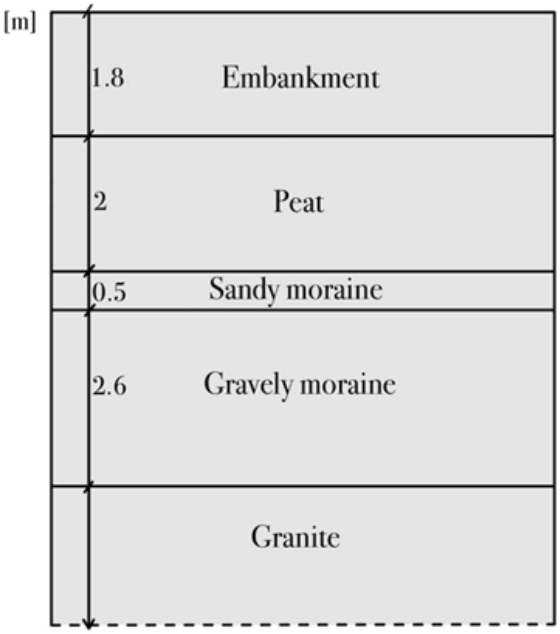
A first challenge was to determine representative effective stiffnesses for the different support areas. A physically based determination would require detailed FEM simulations of the individual structural layers under representative loading conditions, followed by homogenisation of their combined response. Such an analysis was outside the scope of the present study. Instead, a simplified estimate of the relative effective stiffness between the two areas was obtained by representing the individual layers as springs in series. Using this approach, the effective stiffness of area 3 was estimated to be approximately 58.7 times higher than that of area 5. Area 5 was assigned a stiffness of 80 MPa, corresponding to the order of magnitude of the embankment stiffness reported for the project, resulting in an effective stiffness of approximately 4.7 GPa for area 3.

The modular DEM-FEM railway model developed in chapter 3 was subsequently adapted to the Högsjö case. The model represents a single moving vehicle load using the moving mass formulation and includes the developed FEM boundary extensions. The support stiffness varies longitudinally between 80 MPa and 4.7 GPa to represent the transition between the two support conditions. Two operating speeds were considered: 125 km/h (35 m/s) for the main track and 70 km/h (20 m/s) for the passing track. An overview of the adapted simulation model is shown in Figure 7.2.

To investigate the influence of the transition design, three characteristic stiffness variations were considered, as shown in Figure 7.3. The linear variation represents an ideal gradual transition between the two support conditions. The sigmoid variation represents an inter-



Soil layer	Thickness $[m]$	Density $[kg/m^3]$	Youngs modulus $[MPa]$	Porosity [-]	Poissons ratio [-]
Embankment	1.8	1800	50	0.3	0.25
Granite	inf & 8.2	3000	70 000	0.3	0.25



Soil layer	Thickness $[m]$	Density $[kg/m^3]$	Youngs modulus $[MPa]$	Porosity [-]	Poissons ratio [-]
Embankment	1.8	1800	50	0.3	0.25
Peat	2	1000	1	0.3	0.25
Sandy moraine	0.5	2000	20	0.3	0.25
Gravely moraine	2.6	2000	40	0.3	0.25
Granite	inf & 3.1	3000	70 000	0.3	0.25

Figure 7.1. Visualisation and properties of the layers of area 3 (left) and area 5 (right) based on the project report [29].

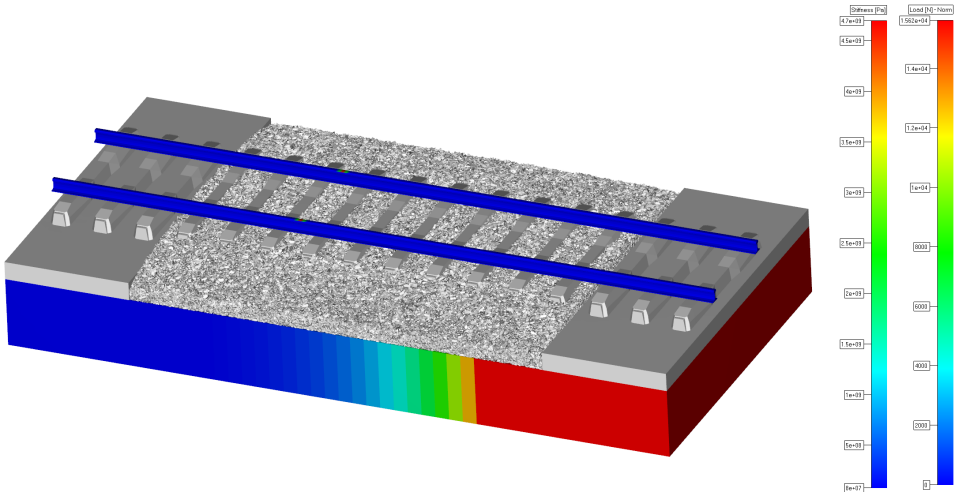


Figure 7.2. Overview of the simulation model applied to Högsjö Västra. The colour scale for the subground shows the variation in stiffness, while the colour scale for the rails shows the moving load.

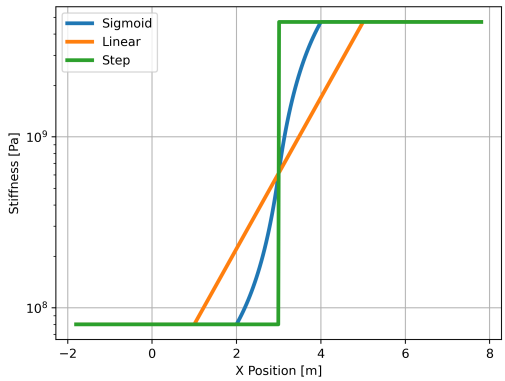


Figure 7.3. Three characteristic stiffness variations considered for the Högsjö transition-zone case.

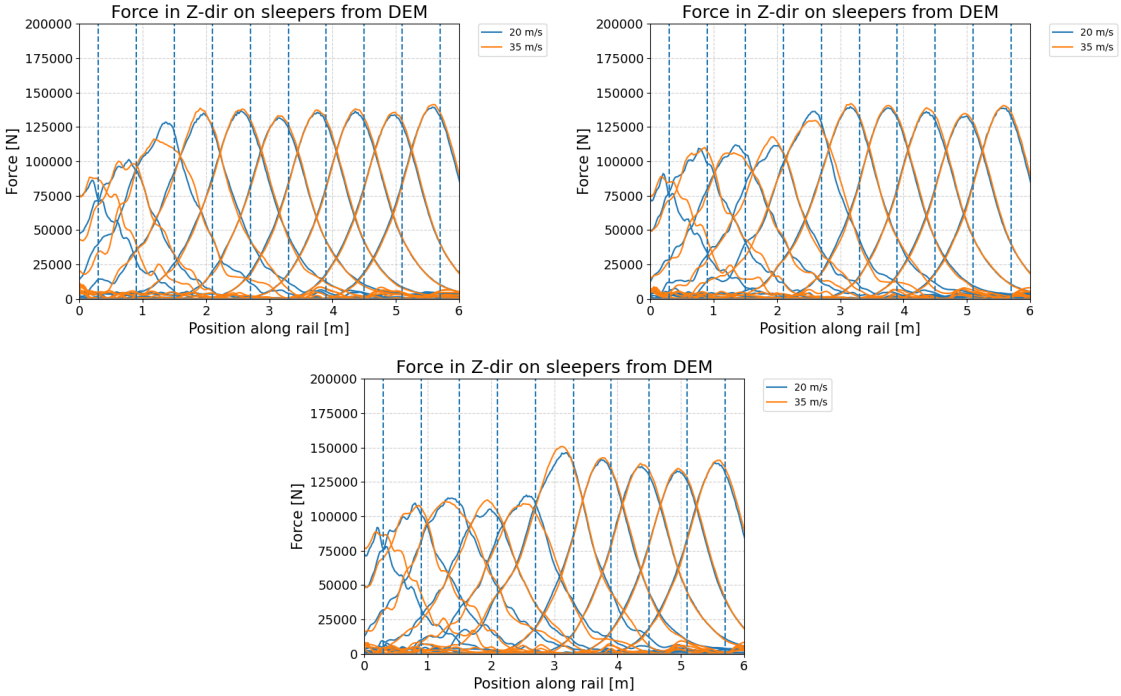


Figure 7.4. Forces acting on individual sleepers for the three considered stiffness variations: linear (top left), sigmoid (top right), and step (bottom). Results for both travelling speeds are shown.

mediate transition design, while the step function represents an abrupt change in support stiffness. The three transition types were evaluated at both operating speeds, resulting in six simulation configurations.

7.1.2. Results

The resulting forces acting on the individual sleepers were evaluated to assess the influence of the transition design on the dynamic track response. The sleeper forces for the two speeds are shown in Figure 7.4 in three subfigures corresponding to each stiffness configuration. The dashed lines indicate the sleeper positions, and the peaks in the force response correspond to the passage of the moving load over the respective sleeper.

The overall force levels are similar for the three transition types. However, clear differences can be observed in the local force response at the transition. The linear stiffness variation produces the smoothest response, with comparatively consistent sleeper forces throughout the transition. In contrast, both the sigmoid and step transitions produce a local increase in sleeper force near the region with the largest stiffness gradient. The peak is higher for

the abrupt step transition than for the sigmoid transition, indicating that an intermediate transition design can already reduce the magnitude of the dynamic force increase.

The comparison between the two travelling speeds shows the same general behaviour for both cases, while the higher speed results in somewhat higher peak forces. The influence of the transition shape is therefore maintained across the two investigated operating conditions.

The results demonstrate the potential of the DEM-FEM framework to evaluate how different transition zone stiffness profiles influence the dynamic response of the track. In particular, the simulations indicate that a gradual change in support stiffness results in a smoother load transfer, whereas an abrupt stiffness change produces a pronounced local force increase. The results further suggest that an intermediate transition profile, such as the sigmoid variation considered here, can reduce the severity of this response without requiring a completely linear transition.

7.1.3. Limitations and future development

The Högsjö case demonstrates the applicability of the developed DEM-FEM framework to a realistic railway infrastructure planning context, but the present study also identifies several areas requiring further development before the approach can be used for detailed engineering design. In particular, a more rigorous workflow is required for determining the effective stiffness of complex support structures. Rather than estimating the relative stiffness from simplified spring models, the effective response of the individual structural layers should be determined from detailed numerical or experimental analyses and subsequently transferred to the idealised transition zone model.

The simplified transition zone representation should also be further evaluated against longer track segments and more detailed representations of the supporting structure. Future work could include the explicit modelling of the relevant structural layers and their actual geometries, allowing the influence of the simplification on the predicted track response to be quantified. Furthermore, the moving mass formulation should be extended towards a more detailed vehicle representation, for example through a multi-body bogie model, to provide a more realistic description of vehicle-track interaction.

These developments would allow the framework to progress from a proof-of-concept application towards a more comprehensive engineering workflow for evaluating and optimising railway transition-zone designs.

8. Conclusions and Recommendations

8.1. Conclusions

The DigiRail project has developed and evaluated a high-performance computational framework for the physics-based simulation of railway infrastructure and the machinery interacting with it. A central objective has been to move beyond isolated component models and instead represent the railway system through coupled numerical descriptions in which granular materials, structural components and mechanical systems can interact. The resulting framework combines the Discrete Element Method (DEM), the Finite Element Method (FEM) and Multi-Body Dynamics (MBD), supported by automated model generation, calibration workflows and high-performance computing.

A coupled DEM–FEM railway model was established in which railway ballast is resolved at particle scale while rails, sleepers and structural components are represented using finite elements. The work demonstrated that modelling choices that are often simplified in large-scale railway simulations can have a significant influence on the calculated response. In particular, non-convex ballast representations resulted in increased interlocking, higher coordination numbers, increased vertical stiffness and reduced accumulated settlement compared with convex representations. Dedicated FEM boundary extensions were also shown to substantially reduce artificial end effects in finite track models. Together with stochastic rail irregularities and a moving-mass formulation, these developments provide a more realistic basis for analysing dynamic railway loading and transition zones.

The project has placed substantial emphasis on experimental validation at different scales. Large-scale vibratory roller experiments were reproduced using coupled DEM–MBD simulations over a sequence of 14 roller passes. The model captured the principal evolution of accumulated settlement and major characteristics of the measured ground-pressure response. The simulations additionally provided information that is difficult to obtain experimentally, including the evolution of packing density with depth. This illustrates an important role for detailed numerical simulation: not only reproducing measurable quantities, but also exposing internal mechanisms that can support interpretation and optimisation of construction processes.

The general DEM–MBD coupling methodology was further evaluated against full-scale wheel-loader experiments. For several investigated operating sequences, the simulations reproduced important characteristics of bucket filling, pile deformation and machine response, while other cases revealed limitations associated with the simplified machine model. The results therefore both validate important aspects of the co-simulation methodology and demonstrate the need for application-specific validation when increasingly complex machine–material interactions are considered.

Railway-specific ballast validation was performed through large-scale sleeper push tests and cyclic oedometer experiments. The combined experimental and numerical results showed that particle size distribution influences ballast deformation, stiffness and degradation, while confinement and applied vertical loading have a particularly strong influence on mobilised lateral resistance. The DEM models reproduced the principal trends between the investigated materials and provided particle-scale explanations through differences in contact

networks and load transmission. The experiments also demonstrated that gradings exhibiting similar macroscopic shear strength may differ substantially in permanent deformation and degradation behaviour.

At structural scale, coupled DEM–FEM simulations of the experimental trough bridge reproduced the order of magnitude and overall distribution of ballast-induced pressure on the bridge structure. The simulations further demonstrated that different realizations of nominally identical ballast beds can produce asymmetric and spatially varying load paths. This result highlights a feature that is difficult to represent using conventional deterministic load-distribution assumptions and indicates that the stochastic granular structure of ballast may be relevant when local structural loads are considered.

For railway maintenance, a coupled DEM–MBD model of ballast tamping was developed and calibrated against operational data from a fully hydraulic tamping system. Within the investigated numerical cases, the hydraulic tamping concept produced a combination of high packing density and lower exposure to large particle forces compared with the simulated conventional system. These results indicate the potential of coupled simulation for analysing both maintenance effectiveness and material loading, although additional experimental validation and explicit modelling of ballast degradation are required before quantitative conclusions regarding long-term ballast damage can be drawn.

Finally, the developed railway model was applied to a transition-zone case based on the Högsjö Västra project. The simulations showed that the longitudinal distribution of support stiffness influences the local dynamic load transfer between the vehicle, track and supporting structure. Gradual stiffness variations produced a smoother sleeper-force response than an abrupt stiffness change, while an intermediate transition profile reduced the local force increase compared with the step transition. The study should presently be regarded as a proof of concept: further work is required to determine effective support stiffnesses using more rigorous methods, to validate the transition-zone response against measurements and to introduce more detailed vehicle dynamics.

Taken together, the project demonstrates that coupled DEM–FEM–MBD simulation has progressed from primarily method-oriented development towards application at scales and configurations relevant to railway engineering. The strongest current capability is the mechanistic analysis of problems in which the discrete behaviour of ballast or other coarse granular materials interacts with structures or machinery and cannot readily be represented by conventional continuum approaches alone. The work also shows that detailed physics-based simulations should complement, rather than replace, established engineering calculation methods. Their principal value is the ability to investigate mechanisms, quantify the consequences of modelling assumptions, evaluate new concepts and provide information that is difficult or impossible to obtain directly from experiments.

8.2. Recommendations

The next stage of development should place continued emphasis on validation and on connecting the detailed numerical models more directly to engineering decision-making. In particular, transition-zone modelling would benefit from a systematic methodology for deriving effective support stiffness from layered soil and structural models, followed by validation against instrumented full-scale railway sites. A more detailed vehicle model should be introduced where vehicle–track interaction contributes significantly to the dynamic response.

Further development of the ballast model should include particle degradation and breakage. Several of the investigations in DigiRail demonstrate that particle-scale loading, particle shape and grading influence the long-term response, but degradation is currently represented primarily through experimental observations or indirect numerical indicators. Introducing calibrated breakage models would enable construction, operational loading and maintenance to be studied within a more consistent lifecycle framework.

Uncertainty and natural variability should also be treated explicitly. The trough-bridge simulations demonstrate that different particle arrangements can produce different local load distributions even for nominally identical material and boundary conditions. Future engineering studies should therefore consider ensembles of granular realizations and statistical descriptions of the predicted response rather than relying exclusively on individual deterministic simulations.

For construction and maintenance machinery, continued use of modular co-simulation through standardised interfaces is recommended. This enables detailed DEM descriptions to be combined with machine models developed in established MBD environments while retaining clear separation between the individual numerical components. Further experimental campaigns should be designed specifically to validate both machine dynamics and granular response under the operating conditions for which the models are intended to be used.

Finally, the automated modelling, calibration and high-performance computing workflows established within DigiRail should be maintained and developed as a common simulation platform. Continued emphasis should be placed on parameterised model generation, reproducible simulation studies and interfaces that allow detailed research models to be translated into practical engineering workflows. This provides a route towards using physics-based simulation not only for research, but also as a quantitative tool for evaluating alternative materials, structural concepts, construction processes and maintenance strategies.

References

[1] European Rail Research Advisory Council (ERRAC). *Rail 2050 Vision*. Tech. rep. European Rail Research Advisory Council, Dec. 2017.

[2] Annika Canaki and Ulrika Honauer. *Trafikverkets underhållsplan för åren 2023–2026*. Tech. rep. 2023:019. Ärendenummer TRV 2023/13380. Trafikverket, May 2023.

[3] Kristina Gustafsson. *Trafikverkets forsknings- och innovationsplan för åren 2024–2029*. Tech. rep. 2024:001. Ärendenummer TRV 2023/133492. Trafikverket, 2024.

[4] W. L. Lim and G. R. McDowell. "Discrete element modelling of railway ballast". In: *Granular Matter* 7.1 (2005), pp. 19–29. DOI: 10.1007/s10035-004-0189-3.

[5] Nishant Kumar, Bettina Suhr, Stefan Marschnig, Peter Dietmaier, Christof Marte, and Klaus Six. "Micro-mechanical investigation of railway ballast behavior under cyclic loading in a box test using DEM: effects of elastic layers and ballast types". In: *Granular Matter* 21.4 (2019), p. 106. DOI: 10.1007/s10035-019-0956-9.

[6] Qiusheng Gu, Chuang Zhao, Xuecheng Bian, John Paul Morrissey, and Jin Yeam Ooi. "Trackbed settlement and associated ballast degradation due to repeated train moving loads". In: *Soil Dynamics and Earthquake Engineering* 153 (2022), p. 107109. DOI: 10.1016/j.soildyn.2021.107109.

[7] Yahia Alabbasi and Mohammed Hussein. "Geomechanical Modelling of Railroad Ballast: A Review". In: *Archives of Computational Methods in Engineering* 28.3 (2021), pp. 815–839. DOI: 10.1007/s11831-019-09390-4.

[8] Cheng Chen and Glenn R. McDowell. "An investigation of the dynamic behaviour of track transition zones using discrete element modelling". In: *Proceedings of the Institution of Mechanical Engineers, Part F: Journal of Rail and Rapid Transit* 230.1 (2016), pp. 117–128. DOI: 10.1177/0954409714528892.

[9] Can Shi, Chunfa Zhao, Yang Yang, Yunlong Guo, Xu Zhang, and Yang Feng. "Macro-meso dynamic analysis of railway transition zone: Hybrid DEM/FDM simulation and experimental validation". In: *Soil Dynamics and Earthquake Engineering* 135 (2020), p. 106191. DOI: 10.1016/j.soildyn.2020.106191.

[10] P. A. Cundall and O. D. L. Strack. "A discrete numerical model for granular assemblies". In: *Géotechnique* 29.1 (1979), pp. 47–65. DOI: 10.1680/geot.1979.29.1.47.

[11] Jan Eliáš. "Simulation of railway ballast using crushable polyhedral particles". In: *Powder Technology* 264 (2014), pp. 458–465. DOI: 10.1016/j.powtec.2014.05.052.

[12] F. Lanaro and P. Tolppanen. "3D characterization of coarse aggregates". In: *Engineering Geology* 65.1 (2002), pp. 17–30. DOI: 10.1016/S0013-7952(01)00133-8.

[13] François Nader, Patrick Pizette, Nicolin Govender, Daniel Wilke, and Jean-François Ferellec. "Modelling realistic ballast shape to study the lateral pull behaviour using GPU computing". In: *EPJ Web of Conferences* 249 (2021), p. 06003. DOI: 10.1051/epjconf/202124906003.

[14] Nicolin Govender, Daniel N. Wilke, Schalk Kok, and Rosanne Els. "Development of a convex polyhedral discrete element simulation framework for NVIDIA Kepler based GPUs". In: *Journal of Computational and Applied Mathematics* 270 (2014), pp. 386–400. DOI: 10.1016/j.cam.2013.12.032.

[15] Adam Bilock. "A GPU Polyhedral Discrete Element Method: Formulation and implementation of large scale simulations for irregular non-convex particles using novel GPU techniques". Master's thesis. Chalmers University of Technology, 2020.

[16] Weimin Song, Baoshan Huang, Xiang Shu, Jan Stránský, and Hao Wu. "Interaction between Railroad Ballast and Sleeper: A DEM-FEM Approach". In: *International Journal of Geomechanics* 19.5 (2019), p. 04019030. DOI: 10.1061/(ASCE)GM.1943-5622.0001388.

[17] Anita Ullrich. "Development of a DEM-FEM framework for infrastructure simulations". Master's thesis. University of Gothenburg, Department of Physics, 2022.

[18] Shunwei Shi, Liang Gao, Xiaopei Cai, Hao Yin, and Xiangning Wang. "Effect of tamping operation on mechanical qualities of ballast bed based on DEM-MBD coupling method". In: *Computers and Geotechnics* 124 (2020), p. 103574. DOI: 10.1016/j.compgeo.2020.103574.

[19] Carl Wersäll, Ingmar Nordfelt, and Stefan Larsson. "Resonant roller compaction of gravel in full-scale tests". In: *Transportation Geotechnics* 14 (2018), pp. 93–97. DOI: 10.1016/j.trgeo.2017.11.004.

[20] Silvia Sarmiento, Jaime Gonzalez-Libreros, Chao Wang, Lennart Elfgren, Ola Enoksson, Tommy Höjsten, Lars-Olof Andersson, and Gabriel Sas. "Experimental and reliability analyses for fatigue-induced damage in reinforced concrete trough bridges". In: *Case Studies in Construction Materials* (2025), e05319.

[21] Wenli Jia, Valeri Markine, Yunlong Guo, and Guoqing Jing. "Experimental and numerical investigations on the shear behaviour of recycled railway ballast". In: *Construction and Building Materials* 217 (Aug. 2019), pp. 310–320. ISSN: 0950-0618. DOI: 10.1016/j.conbuildmat.2019.05.020.

[22] Alireza Ahmadi, Carl Wersäll, and Stefan Larsson. "Impact of particle arrangement and model dimensions on DEM modeling of high-speed railway ballasted tracks in 2D and 3D". In: *Transportation Geotechnics* 47 (July 2024), p. 101272. ISSN: 2214-3912. DOI: 10.1016/j.trgeo.2024.101272.

[23] Anita Ullrich, Johannes Quist, Gustav Kettil, and Magnus Ekh. "On the Influence of Non-Convex Particles in DEM-FEM Simulations of Railway Tracks". In: (2026). Preprint available at SSRN 6603995. DOI: 10.2139/ssrn.6603995.

[24] M Podwórna. "Modelling of random vertical irregularities of railway tracks". In: *International Journal of Applied Mechanics and Engineering* 20.3 (2015).

[25] Johannes Quist, Klas Jareteg, Adam Bilock, and Andreas Persson. *Undersökning av separationseffekter vid kompaktering av obundna material*. Final report SBUF Projekt 13820. 2021. URL: https://www.sbuf.se/projektresultat/projekt?id=005ad6c4-5b0a-4a78-a991-aadabad36a79.

[26] Johannes Quist, Pontus Malmsköld, Anita Ullrich, Caroline Ansin, Kristoffer Hofling, Andreas Persson, Christoffer Brauer, and Mikael Knutsson. "Evaluation of Alternative Particle Size Distributions for Railway Ballast". In: *SBUF projectnr. 14488* (2026-04-30).

[27] Silvia Sarmiento. "Remaining service life estimation of existing concrete bridges through probabilistic and reliability analyses". PhD thesis. Luleå University of Technology, 2025.

[28] Alex Eriksson, Anita Ullrich, Chao Wang, Jaime Gonzalez-Libreros, Johan Johansson, Ola Enoksson, Johannes Quist, and Gabriel Sas. "Numerical and Analytical Evaluation of Load Distribution Patterns on Ballasted Concrete Railway Bridges". In: *Building for the Future: Durable, Sustainable, Resilient: Proceedings of the fib Symposium 2023-Volume 2.*: Springer Nature Switzerland, 2023, pp. 109–118. DOI: 10.1007/978-3-031-32511-3_12.

[29] Simon Jobäck and Hanan Sabri. *Dynamic soil response to high speed rail*. Master's Thesis. Chalmers University of Technology. 2025.